doi:10.1111/evo.12534

Evolutionary bursts in *Euphorbia* (Euphorbiaceae) are linked with photosynthetic pathway

James W. Horn,[1] Zhenxiang Xi,[2] Ricarda Riina,[3,4] Jess A. Peirson,[3] Ya Yang,[3] Brian L. Dorsey,[3,5] Paul E. Berry,[3] Charles C. Davis,[2] and Kenneth J. Wurdack[1,6]

[1]*Department of Botany, Smithsonian Institution, NMNH MRC-166, P.O. Box 37012, Washington, DC 20013*

[2]*Department of Organismic and Evolutionary Biology, Harvard University Herbaria, 22 Divinity Avenue, Cambridge, Massachusetts 02138*

[3]*Department of Ecology and Evolutionary Biology and University of Michigan Herbarium, 3600 Varsity Drive, Ann Arbor, Michigan 48108*

[4]*Real Jardín Botánico, RJB-CSIC, Plaza de Murillo 2, 28014 Madrid, Spain*

[5]*The Huntington Botanical Gardens, 1151 Oxford Road, San Marino, California 91108*

[6]*E-mail: wurdackk@si.edu*

Received December 6, 2013
Accepted September 17, 2014

The mid-Cenozoic decline of atmospheric CO_2 levels that promoted global climate change was critical to shaping contemporary arid ecosystems. Within angiosperms, two CO_2-concentrating mechanisms (CCMs)—crassulacean acid metabolism (CAM) and C_4—evolved from the C_3 photosynthetic pathway, enabling more efficient whole-plant function in such environments. Many angiosperm clades with CCMs are thought to have diversified rapidly due to Miocene aridification, but links between this climate change, CCM evolution, and increased net diversification rates (*r*) remain to be further understood. *Euphorbia* (~2000 species) includes a diversity of CAM-using stem succulents, plus a single species-rich C_4 subclade. We used ancestral state reconstructions with a dated molecular phylogeny to reveal that CCMs independently evolved 17–22 times in *Euphorbia*, principally from the Miocene onwards. Analyses assessing among-lineage variation in *r* identified eight *Euphorbia* subclades with significantly increased *r*, six of which have a close temporal relationship with a lineage-corresponding CCM origin. Our trait-dependent diversification analysis indicated that *r* of *Euphorbia* CCM lineages is approximately threefold greater than C_3 lineages. Overall, these results suggest that CCM evolution in *Euphorbia* was likely an adaptive strategy that enabled the occupation of increased arid niche space accompanying Miocene expansion of arid ecosystems. These opportunities evidently facilitated recent, replicated bursts of diversification in *Euphorbia*.

KEY WORDS: **Ancestral state reconstruction, C_4 photosynthesis, CAM photosynthesis, climate change, diversification, Miocene, species selection, succulent.**

It is becoming apparent that the success of angiosperms is associated with increases in species net diversification (speciation minus extinction) rates among numerous, highly nested clades within the flowering plant tree-of-life (Smith et al. 2011). Although the drivers of these evolutionary bursts are likely to be stochastic in some cases, interpreting these events in terms of interactions between intrinsic (key innovations) and extrinsic factors (key opportunities) remains a viable framework for explaining these patterns (de Queiroz 2002; Vamosi and Vamosi 2011; Givnish et al. 2014). The results of recent divergence time estimates of land plants, when integrated with paleoclimatic and paleoecological data, point to climate change as a "key

EVOLUTION
INTERNATIONAL JOURNAL OF ORGANIC EVOLUTION

opportunity" insofar as it creates novel niche space over time (Ackerly 2009; Shaw et al. 2010; Bytebier et al. 2011; Pittermann et al. 2012). A striking and increasingly well-studied example of climate change creating novel ecological opportunity centers on the mid-Miocene (~14 Ma), when cooling and aridification (Zachos et al. 2001) coincided with sharply decreased atmospheric CO_2 concentrations (Beerling and Royer 2011). Indeed, global CO_2 levels may have reached a near record low in the late Miocene (~8 Ma; Tripati et al. 2009), continuing a trend that began in the early Oligocene (~30 Ma; Pagani et al. 2005). Regional intensification of this aridification occurred on all continents in the late Miocene through the Pliocene and is thought to have advanced the relatively rapid development of modern arid ecosystems and tropical grasslands (Cerling et al. 1993, 1997; Arakaki et al. 2011; Pound et al. 2012), due to a confluence of global atmospheric changes with regional scale changes in oceanic currents and tectonic events (Suc 1984; Partridge 1993; Ruddiman and Kutzbach 1989; Guo et al. 2004; Jacobs 2004; Sepulchre et al. 2006; Eronen et al. 2012).

Alternative photosynthetic pathways (e.g., crassulacean acid metabolism [CAM] and C_4), here termed CO_2-concentrating mechanisms (CCMs), can be viewed as a putative "key innovation" (Simpson 1953). In a low CO_2 world, CCMs confer adaptive benefits to plants in arid environments that enhance their competitive ability relative to C_3 plants (de Queiroz 2002; Herrera 2009), suggesting a link between CCMs and increased net diversification. We find this idea compelling to explain at least some of the historical contingency that may account for more recent instances of exceptional angiosperm diversification. The reasons for this interpretation are that (1) CCMs confer increased photosynthetic capacity and water-use efficiency (WUE) in arid environments (Cushman 2001; Osborne and Beerling 2006; Kadereit et al. 2012; Osborne and Sack 2012; Pau et al. 2013), (2) CCMs have numerous, independent origins within angiosperms (Smith and Winter 1996; Silvera et al. 2010; Sage et al. 2011a; Edwards and Ogburn 2012), and (3) CCM plants exhibit a high degree of dominance in contemporary dryland ecosystems (Lüttge 2004; Sage 2004; Edwards and Smith 2010; Alvarado-Cárdenas et al. 2013). Furthermore, divergence time estimates of major angiosperm clades in which CCMs are present suggest that the timing of diversification rate increases in these clades is consistent with the hypothesis that Miocene/Pliocene aridification was an important extrinsic driver of these events (Klak et al. 2004; Good-Avila et al. 2006; Arakaki et al. 2011; Hernández-Hernández et al. 2014; Spriggs et al. 2014).

An important aspect of CCM lineage evolution that is not well understood is the relationship between the environmental drivers of CCM origins and the arid biome expansion that is linked to increased diversification in some CCM lineages. Because aridity is implicated in both phenomena (Edwards and Ogburn 2012), understanding the temporal relationship between them is critical for discriminating among competing hypotheses of paleoenvironmental drivers, as Spriggs et al. (2014) demonstrate for C_4 grasses. To further illuminate the relationship between time, CCM origins, and both among-lineage and trait-dependent diversification in a lineage in which CCMs have a complex evolutionary history, we present analyses addressing these evolutionary questions in the large and globally distributed clade *Euphorbia* (Euphorbiaceae).

Euphorbia contains ~2000 species and is a key component of arid ecosystems worldwide, especially in the tropics (Horn et al. 2012). Because of its unique flower-like inflorescence, the cyathium, *Euphorbia* has been recognized as a natural group and in its current broad circumscription is monophyletic. *Euphorbia* species are components of most types of terrestrial biomes, but are most abundant in warm, seasonally dry, and arid ecosystems where they manifest an unusually large range of growth forms (Fig. 1A, D, G). The genus is well known for its ~850 xerophytic species, largely consisting of diverse stem succulents that use CAM photosynthesis (Fig. 1G; McWilliams 1970; Bender et al. 1973; Webster et al. 1975; Mooney et al. 1977; Winter 1979). Among these succulents are the famous African analogs to the New World cacti and the many "pencil-stemmed" species, including the familiar pencil tree, *E. tirucalli*. The principally New World radiation of section *Anisophyllum* (formerly recognized as the genus *Chamaesyce*) consists of ~365 species and is also biologically distinctive because they are commonly weedy C_4 herbs with strongly dorsiventral shoot symmetry (Fig. 1D; Yang and Berry 2011; Horn et al. 2012).

Previous ideas concerning the evolution of *Euphorbia* centered on the origin of the cyathium as a key innovation because of its importance for enabling a putative switch from wind to insect pollination, which, in turn, promoted increased speciation rates (Webster 1967; Prenner and Rudall 2007). Contemporary phylogenetic and comparative studies of *Euphorbia*, however, reveal strong asymmetries in species richness among sectional subclades within each of the four subgeneric *Euphorbia* clades—a pattern suggesting contrasted among-lineage diversification rates within the genus (Steinmann and Porter 2002; Zimmerman et al. 2010; Bruyns et al. 2011; Horn et al. 2012; Yang et al. 2012; Dorsey et al. 2013; Peirson et al. 2013; Riina et al. 2013). Correspondingly, divergence time estimates of *Euphorbia* indicate that many large sectional subclades characterized by CCMs may be relatively young (van Ee et al. 2008; Bruyns et al. 2011). A synthesis of this information suggests that possible evolutionary bursts in *Euphorbia* may be more closely linked to intrinsic drivers other than the origin of the cyathium and, in particular, points to a link between some of these apparent bursts of diversification and the presence of CCMs in these lineages.

CAM and C_4 photosynthesis (CCMs) separate the process of initial, atmospheric CO_2 fixation from the RuBisCO-mediated

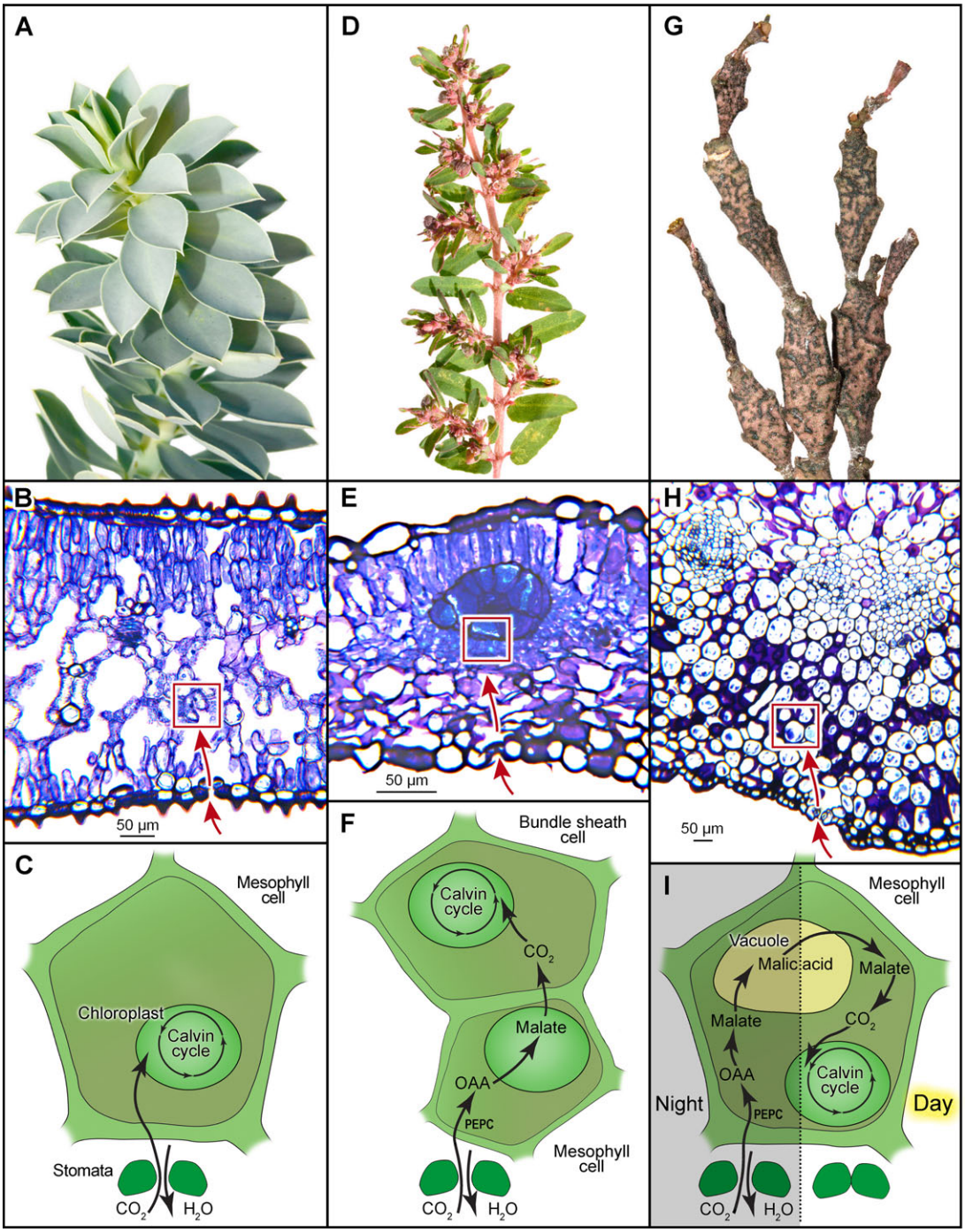

Figure 1. Structural and biochemical features of photosynthetic system type in *Euphorbia*. C_3 species, *Euphorbia myrsinites* (subgenus *Esula*, section *Myrsiniteae*). (A) Leafy shoot. (B) Leaf lamina in transverse section, showing large intercellular air spaces in spongy mesophyll. (C) Schematic of (B) detailing typical C_3 biochemistry in context of structure. C_4 species, *Euphorbia maculata* (subgenus *Chamaesyce*, section *Anisophyllum*). (D) Leafy shoot system. (E) Leaf lamina in transverse section. Note relatively enlarged bundle sheath cells with densely packed organellar contents. (F) Schematic of (E) detailing typical C_4 biochemistry in context of structure. CAM species, *Euphorbia platyclada* (subgenus *Chamaesyce*, section *Bosseriae*). (G) Succulent shoots. (H) Succulent shoot in transverse section, showing stem cortex with densely packed cells, minimizing intercellular air spaces. (I) Schematic of H detailing typical CAM biochemistry in context of structure and time; note temporally inverted stomatal cycle.

Calvin cycle—the reactions constituting C_3 photosynthesis. To do this, both CCMs rely on essentially the same biochemical pathway, in which the enzyme phosphoenolpyruvate carboxylase (PEPC) fixes atmospheric CO_2 with PEP to form the four-carbon acid oxaloacetate (OAA), which is then reduced to malate in both CAM and C_4 *Euphorbia* species (Gutierrez et al. 1974; Sage et al. 2011b; or aspartate in some C_4 lineages outside of *Euphorbia*). Malate is then decarboxylated, releasing CO_2 to be fixed by the Calvin cycle, but in such a manner that it is concentrated around RuBisCO by either an intracellular, temporal mechanism (CAM; Fig. 1H, I) or an intercellular, spatial mechanism (typical C_4; Fig. 1E, F). Hence, under both CCMs, RuBisCO functions in a microenvironment enriched with CO_2 substrate, which limits its oxygenase activity and inhibits wasteful photorespiration. CCMs can also increase WUE because PEPC has a much higher affinity for CO_2 than RuBisCO, enabling much lower rates of stomatal conductance and concomitantly reducing water loss from transpiration relative to C_3 plants. In obligate CAM plants, WUE is further enhanced by their inverted stomatal cycle (Fig. 1I). These benefits are pronounced in high-temperature, high-light, low-CO_2 environments with limited or seasonal precipitation, where CCM plants have greatly increased photosynthetic capacity and WUE relative to C_3 plants (Winter et al. 2005; Herrera 2009; Osborne and Sack 2012).

Although the differences between C_4 and CAM are well known (Keeley and Rundel 2003), recent hypotheses on the evolution of both CCMs explore the similarities between them, emphasizing the shared biochemical pathway and suggesting that structural and genomic features of a given lineage may ultimately influence which CCM manifests (Sage 2002; Edwards and Ogburn 2012). Indeed, Christin et al. (2014a) demonstrate a similar origin of the PEPC involved in both the C_4 and CAM pathways in Caryophyllales (a clade containing the C_4 amaranths and CAM cacti). Broad-scale phylogenetic evidence supports this hypothesis to the extent that it demonstrates a complex evolutionary history of both CCMs within five angiosperm clades of relatively limited size, one of which is *Euphorbia* (Edwards and Ogburn 2012).

Research conducted by collaborators on the EuphORBia Planetary Biodiversity Inventory (PBI) project (Esser et al. 2009; Riina and Berry 2013) provides a wealth of new information on *Euphorbia* phylogenetics, allowing the placement of virtually every species to a sectional-level clade within the genus (Yang et al. 2012; Dorsey et al. 2013; Peirson et al. 2013; Riina et al. 2013). Using a time-calibrated backbone phylogeny for *Euphorbia* (Horn et al. 2012), combined with newly generated carbon isotope data for nearly every species in this phylogeny and species diversity data derived from specialist knowledge, we herein address the timing of CCM origins and their relationship to increases in species diversification across the clade. To do this, we use a series of ancestral state reconstruction analyses in addition to analyses using MEDUSA (Alfaro et al. 2009), a likelihood-based approach for locating diversification rate shifts on a phylogenetic tree. These results allow us to identify and temporally dissect lineage-specific correspondences between these two phenomena, which enable us to relate them to paleoclimatic information and to investigate a link between CCM origins and increased net diversification. To further test a link between CCMs and diversification, we also conducted both likelihood and Bayesian implementations of the BiSSE method (Maddison et al. 2007) and discuss these results in the context of species selection.

Methods and Materials

TAXONOMIC AND MOLECULAR SAMPLING

Our molecular data matrix of 197 tips is based on the 10-marker *Euphorbia* plus subfamily Euphorbioideae outgroups dataset of Horn et al. (2012), with 23 additional *Euphorbia* taxa (Table S1) selected to represent all but one of the major lineages (sections) within the clade (Yang and Berry 2011; Yang et al. 2012; Dorsey et al. 2013; Peirson et al. 2013; Riina et al. 2013). The monotypic section *Szovitsiae* of *Euphorbia* subgenus *Esula* was excluded because it was hypothesized to be a possible intersectional hybrid (Riina et al. 2013). These additional sequences were inserted into the existing alignment of Horn et al. (2012) without the addition of new gaps; we also excluded the same gaps and regions of ambiguous alignment as in Horn et al. (2012). Data matrices and supporting files are available from the Dryad Digital Repository.

To determine the optimal partitioning scheme and associated best-fit models of sequence evolution, we subdivided the data into the largest number of partitions that could be determined a priori (28 total). We then ran PartitionFinder version 1.0.1 (Lanfear et al. 2012) using the "greedy" heuristic search algorithm, linked branch lengths, and a starting tree topology from the best-scoring ML tree of a GARLI version 2.0 (Zwickl 2006) search in which each genetic marker of the concatenated dataset was partitioned separately. We used the Bayesian information criterion (Schwarz 1978) to select the best-fit model. The results indicated an optimal partitioning scheme of 15 partitions with associated models of evolution (Table S2), which was applied to all subsequent sequence-based analyses.

CARBON ISOTOPE RATIO ($\delta^{13}C$) DETERMINATION

Carbon isotope values were determined for 192 of the 197 tips in the phylogeny, using tissue subsamples of the original DNA sources or herbarium specimens (Table S3). Dried leaf or photosynthetic stem tissue was analyzed with an isotope-ratio mass spectrometer and reference standards of acetanilide and urea

calibrated to L-glutamic acid (USGS40 and USGS41). See the Methods section of Supporting Information for additional details.

CALIBRATION

Fossil remains attributable to *Euphorbia* (Friis and Crepet 1987; Anderson et al. 2009) lack sufficient detail to be used as credible calibration points. Our approach to calibrating the divergence dating analysis was based on one fossil calibration point attributable to the outgroup tribe Hippomaneae of Euphorbioideae (*Hippomanoidea warmanensis*, Crepet and Daghlian 1982) and two secondary calibration points within the clade of Euphorbioideae (based on Xi et al. 2012). See the Methods section of Supporting Information for further details.

PHYLOGENETIC AND DIVERGENCE TIME ESTIMATION

An analysis to assess conflict among the 15 partitions of our dataset was not conducted because of its strong similarity with the dataset of Horn et al. (2012), who demonstrated broad congruence between individual partitions, each defined by one of the 10 molecular markers. Our dataset was, likewise, analyzed using a "total evidence" approach (Kluge 1989).

Absolute divergence times and phylogeny for the sampled species were simultaneously estimated using Bayesian Markov Chain Monte Carlo (MCMC) methods with an uncorrelated log-normal relaxed clock (UCLD) model in BEAST version 1.7.4 (Drummond et al. 2006, 2012). Substitution models (Table S2) were unlinked, and clock and tree models were linked among partitions. We set useAmbiguities to "true" for each partition to have BEAST treat ambiguity codes exactly as specified in the matrix. A birth–death process with incomplete sampling (Stadler 2009) and a user-defined starting tree were used for the tree prior. Our starting tree was the optimal GARLI ML tree of the 15-partition dataset transformed in TreeEdit version 1.0a10 (Rambaut and Charleston 2002) to an ultrametric tree using the nonparametric rate smoothing (Sanderson 1997) option, weighting the rate differences at all nodes with the mean, and subsequently scaling the height of the tree to 69.08. Four separate MCMC chains of 6×10^7 generations were initiated and sampled every 1000 generations. We used Tracer version 1.5 (Rambaut and Drummond 2007) to assess convergence between the chains and ensure an effective sample size of >200 was obtained for all parameters. A randomly selected subset of 1000 post burn-in trees was used in all subsequent comparative analyses.

AMONG-LINEAGE DIVERSIFICATION RATE ANALYSES

To assess among-lineage variation in net diversification rates (r), we used MEDUSA (Alfaro et al. 2009; version 0.93-4-33, J. W. Brown, pers. comm.). The MEDUSA method (Alfaro et al. 2009; Santini et al. 2009; Slater et al. 2010) extends an approach developed by Rabosky et al. (2007) of estimating per-lineage diversification rates using taxonomic (species richness) and phylogenetic information by sequentially testing a series of rate and model shifts to a diversity tree until there is no significant improvement in AIC score (Akaike information criterion; Akaike 1974). Because uncertainties in divergence dating estimations can confound estimates of diversification rates, we conducted this analysis using the subset of 1000 chronograms. To do this, we pruned the subset of chronograms to 104 tips of exemplar species to create a set of diversity trees that would maximize robustly supported phylogenetic information and also accurately reflect clade diversity estimates for the total species diversity of Euphorbioideae (excepting section *Szovitsiae*). Details of diversity tree construction are further elaborated in Supporting Information methods. We used an AICc threshold of 4.84, as determined by the program given the size of the initial tree and corresponding richness information, to infer the number of rate shifts in each tree. We ran MEDUSA with starting parameters set so that the choice of speciation model type (Yule or birth–death) and values of r and relative extinction rate (ε) are allowed to vary. The multiMEDUSA function enabled us to tabulate and summarize the results of the 1000 MEDUSA analyses onto the maximum clade credibility tree from the BEAST analysis, which we pruned to 104 tips like the diversity trees. To be conservative in our interpretation of these results, we consider shifts modeled in >50% of the subset of 1000 diversity trees as significant.

ANCESTRAL STATES AND CORRELATES OF DIVERSIFICATION

Using our $\delta^{13}C$ isotope data, we examined the evolution of CCMs and tested the hypothesis that the origin of this physiological novelty is a correlate of increased net diversification rates in *Euphorbia*.

Owing to the need for discrete, binary character data to implement other analyses, we binned the $\delta^{13}C$ values into two character states. We scored photosynthetic pathway with the following states: (0) C_3 (and C_2) pathway(s), where atmospheric CO_2 is directly fixed by RuBisCO; and (1) CCM (CAM and C_4), where atmospheric CO_2 is fixed by PEPC. PEPC discriminates far less against incorporating ^{13}C in carboxylation reactions than does RuBisCO because of differences in enzyme kinetics (Bender 1971; Farquhar et al. 1989). The $^{13}C/^{12}C$ ratio in photosynthetic tissues of terrestrial plants that fix atmospheric CO_2 principally by PEPC is, therefore, much closer to atmospheric levels, which have $\delta^{13}C$ values measured at about −8‰ (Keeling et al. 1979; O'Leary 1988). Signature $\delta^{13}C$ values for typical C_4 plants range from −16‰ to −10‰ and CAM plants typically range from −20‰ to −10‰, whereas $\delta^{13}C$ values for typical C_3 plants range from −33‰ to −22‰ (O'Leary 1988).

PEPC always catalyzes the carboxylation reactions involving atmospheric CO_2 in the intercellular CO_2-fixation mechanism of typical C_4 plants. Correspondingly, the range of $\delta^{13}C$ values recorded for C_4 plants is both relatively narrow and distinct from that of C_3 plants. This is the case in *Euphorbia*, where expression of the C_4 pathway is almost certainly restricted to subsection *Hypericifoliae* of section *Anisophyllum* (Webster et al. 1975; Yang et al. 2012). There are no known reversals back to a putative C_3 pathway in this clade, not even in Hawaiian endemic species that grow in the understory of mesic forests or in high elevation bogs (Pearcy and Troughton 1975).

In contrast, CAM expression is flexible (Winter et al. 2008; Silvera et al. 2010; Borland et al. 2011), with net carbon gain during daytime relative to nighttime having a linear relationship with $\delta^{13}C$ values (Winter and Holtum 2002). Values of $\delta^{13}C$ for plants with CAM cycling or facultative to weak CAM expression frequently lie within the range typical of C_3 plants (Pierce et al. 2002; Silvera et al. 2005); establishing CAM activity in such plants entails more elaborate physiological experiments that require living source material (Silvera et al. 2005; Herrera 2013). Although these weaker modes of CAM expression are likely important for a nuanced understanding of CAM evolution, we were interested in investigating origins of strong to obligate CAM expression in *Euphorbia*.

To account for the inherent subjectivity in using a cutoff value to bin the $\delta^{13}C$ data into discrete character states to distinguish CCM function from a C_3 state, we used three binning schemes defined by cutoff values of $-21‰$, $-20‰$, $-19‰$. This range of $\delta^{13}C$ values corresponds to a range of ~35–50% of net carbon gain during the night for CAM plants (71–77% of net carbon uptake in "typical" CAM plants occurs at night; Winter and Holtum 2002, their Fig. 6A). These cutoff values are consistent with those of other studies employing binning schemes of $\delta^{13}C$ to explore the evolution of CCMs (e.g., Bromeliaceae, $-20‰$: Crayn et al. 2004).

We used the BiSSE model (Maddison et al. 2007), implemented in the R package *diversitree* (FitzJohn 2012), to jointly estimate character state transition rates and state-dependent speciation and extinction rates. To account for incomplete sampling, we used the terminally unresolved clades function (FitzJohn et al. 2009) with the same subset of 1000 diversity trees and corresponding tip diversity information as the MEDUSA analyses. Because we were unable to obtain $\delta^{13}C$ data for all species modeled at each tip, we scored CCM type for unassayed species by extrapolating our $\delta^{13}C$ results from assayed species at each tip to closely related, unassayed species based on structural similarity and, particularly, stem or leaf succulence. As described above, C_4 photosynthesis has a single origin within *Euphorbia*, with probably no transitions back to a C_3 pathway, so our estimates focused on distinguishing species with predominantly C_3 or C_3-like activity from those with strong CAM expression. Hence, succulent relatives of succulent species we determined by carbon isotope analysis as having strong CAM expression were scored as state 1. We could apply this criterion across all study taxa with little ambiguity. Of the 2256 species we modeled in the BiSSE analyses, 51.4% were scored as state 0 and 47.7% were scored as state 1; the remaining 20 species were not scored because of questionable character state assignment and were treated by the program as having missing trait information (Table S4).

The unconstrained BiSSE model consists of six parameters subdivided into three pairs of rate categories: speciation (λ_0, λ_1), extinction (μ_0, μ_1), and character state transition (q_{01}, q_{10}). Seven further submodels may be derived from this model by constraining the values of one or more of the three rate categories as equal, enabling a framework for hypothesis testing or model selection. We conducted ML searches using the subplex optimization procedure for each of the eight possible BiSSE submodels across the 1000 diversity trees to obtain estimates for these parameters. To obtain reasonable estimates of starting values for λ and μ for each tree, we fit a constant rate birth–death model to each tree with unresolved clade information. We also provided starting values of q_{01} and q_{10} for each diversity tree based on estimated transition rates from a two-parameter ML optimization in Mesquite version 2.75 (Maddison and Maddison 2011) of the corresponding 197-tip tree, using $-20‰$ as a cutoff value to provide a binary coding for the $\delta^{13}C$ data. Models were compared using AIC scores and Akaike weights (Burnham and Anderson 2002).

To examine the uncertainty in the BiSSE parameter estimates, we further analyzed the two models in the confidence set from the ML BiSSE analysis using Bayesian MCMC methods in *diversitree*. We modeled the prior for each model with an exponential distribution and a rate of $1/2r$ and a step size that was the range of the observed samples from a preliminary MCMC run of 100 generations. We ran a chain of 15,000 generations for each model using the maximum clade credibility tree from the BEAST analysis, pruned to the same 104 tips as the set of diversity trees, with unresolved clade information. We examined the output of each run to estimate burn-in, ensure convergence, and check for autocorrelation among samples.

We conducted the ancestral state estimations of CCM evolution using ML optimizations (Schluter et al. 1997; Pagel 1999) in Mesquite. To avoid inaccurate transition rate estimates in Mesquite because of incomplete sampling (Goldberg and Igić 2008) and account for transition rate model uncertainty in the results of our ML BiSSE analysis, we used the median rate estimates inferred for the confidence set of models of the ML BiSSE analysis (Table 6) for a two-rate model (asymmetrical two-parameter Markov-k) and a single-rate model (Mk1; Lewis 2001) in conjunction with the three binary coding schemes of the $\delta^{13}C$ data described above. Hence, we conducted separate analyses for each

of the six different transition rate model/binning combinations. To accommodate for phylogenetic and branch length uncertainty, we conducted each of these optimizations using the subset of 1000 197-tip chronograms. A given ancestral state was assigned to a node if its raw likelihood was >2 log units better than the likelihood value of the other state (i.e., default in Mesquite). We then summarized the results onto the 95% majority-rule consensus topology of all post burn-in trees of the BEAST analysis.

Results

PHYLOGENETIC INFERENCE AND DIVERGENCE TIME ESTIMATION

Phylogenetic relationships and branch support values of the Bayesian MCMC analyses for the 197-tip dataset (see Supporting Information Methods and Fig. S1) are similar to those obtained by Horn et al. (2012). Placements of the 23 *Euphorbia* species added to the Horn et al. (2012) matrix are generally congruent with the results of studies using denser taxon sampling that focus on major clades within *Euphorbia* (i.e., Yang and Berry 2011; Yang et al. 2012; Dorsey et al. 2013; Peirson et al. 2013; Riina et al. 2013).

We recovered a median age estimate of 47.8 Ma (95% highest posterior density [HPD]: 41.0–54.7 Ma) for the crown clade of *Euphorbia*. Median and 95% HPD age estimates of the four, successively sister, subgeneric clades that comprise *Euphorbia*—*Esula*, *Athymalus*, *Chamaesyce*, and *Euphorbia*—and also significant clades within the subgenera are given in Table 1 and further depicted in Figures 2 and S2. Compared with the ages recovered by Bruyns et al. (2011) in a genus-wide study that focused on Old World succulent species, our estimate of the age of *Euphorbia* is ∼10 Ma older. The age estimates we recovered for the four subgeneric clades and sectional clades within *Euphorbia* are only broadly congruent with those recovered by Bruyns et al. (2011), with some differing by ±10 Ma relative to our estimates. We suggest our dating results are more accurate than those of Bruyns et al. because of our (1) synoptic taxon sampling; (2) use of improved external calibration point information specific to nodes within Euphorbioideae; (3) use of methods that assume uncorrelated substitution rate variation among adjacent branches, which is critical for reliable dating estimates within clades, such as Euphorbioideae, where substitution-rate heterogeneity is pronounced; and (4) use of several markers with low rate variation (see Horn et al. 2012; Christin et al. 2014b for 3 and 4).

CARBON ISOTOPE RATIO DATA AND ANCESTRAL STATE ESTIMATION OF CCM

Results of the $\delta^{13}C$ analyses (Table S3) reveal a strongly bimodal distribution of values, with the two peaks centered at about −27.5‰ and −16‰ (Fig. S3).

The character histories we obtained using the six different parameter combinations, based on the three $\delta^{13}C$ cutoff values and the two transition model types, were generally congruent (Figs. S4 and S5). They demonstrate that CO_2 fixation principally by the C_3 pathway is the ancestral condition in *Euphorbia* and other Euphorbioideae. Significant CO_2 fixation by CCMs evolved independently within each of the four subgeneric clades of *Euphorbia* (Fig. 2), and a total of 17–22 CCM origins may be inferred using the two-parameter rate model, taking into account the modest variation among the three character histories along with alternative interpretations of character state optimization at nodes with an ambiguous reconstruction (Fig. S4; 13–20 transitions under the one-parameter rate model, Fig. S5). Nodes reconstructed with equivocal states are the greatest source of uncertainty in estimating the number of CCM origins. Ages of transitions to CAM for *Euphorbia* subclades (i.e., excluding transitions in stem lineages of tip species) are predominantly early Miocene to late Pliocene/early Quaternary in age ([34.3–] 22.1–2.2 Ma; [34.3–] 22.1–1.3 Ma, including 95% HPD; Table 2; Fig. 2). The single origin of a fully optimized C_4 pathway in the stem lineage of section *Anisophyllum* subsection *Hypericifoliae* (subgenus *Chamaesyce*) occurred slightly earlier than most CAM origins (Tables 1 and 2; Fig. 2).

SHIFTS IN DIVERSIFICATION RATES

Across the 1000 diversity trees we examined, the MEDUSA analysis modeled a minimum of six rate shifts and maximum of 15 rate shifts, with a mean of 10.54 shifts and median of 10 shifts (Fig. S6). Eight, non-nested rate shifts were modeled in >50% of the diversity trees, all of which represent increases in the net diversification rate (r) relative to background values of r (Tables 3 and 4; Fig. 3). Nine other rate shifts were modeled, with rapidly diminishing frequency, in 10–50% of the diversity trees (Table S5). A birth–death model was initially selected as the best fit for the entire tree in all of the 1000 diversity trees, with the clades associated with the top eight rate shifts subsequently fit with a Yule (pure birth) model. These eight clades are distributed across all four subgeneric clades and collectively contain 1235 of the ∼2000 species of *Euphorbia* (Fig. 3). Mapped increases in r for these clades are generally mid-Miocene (∼15 Ma) or younger in age (Table 1; Fig. 3), and six of the eight clades wholly or largely consist of species with CCMs (Tables 1, 2, and S4; Fig. 2). CCMs originated prior to three of these six rate shifts (shifts 1, 3, and 6) and just after the position of the other three rate shifts (shifts 4, 7, and 8; Table 2; Fig. 2).

A ranking based on ΔAIC and Akaike weights of the eight BiSSE submodels that we tested across the 1000 diversity trees indicates that the two best-fit submodels are those with free speciation and extinction parameters (i.e., the full six-parameter and five-parameter, transition rate constrained submodels; Table 5).

Table 1. Divergence times for *Euphorbia* and its major clades.

Taxon	Median crown age	95% HPD crown age	Median stem age	95% HPD stem age	Area of origin (shifts only)
Euphorbia	47.8	41.0–54.7	54.7	47.5–61.9	
Subgeneric clades					
Esula	40.5	33.2–47.7	47.8	41.0–54.7	
Athymalus	24.6	16.3–33.5	44.7	37.8–51.4	
Euphorbia	30.8	24.6–36.4	39.1	32.9–45.6	
Chamaesyce	36.0	30.3–42.1	39.1	32.9–45.6	
Sectional clades					
***Esula* (5; C_3)**	**8.5**	**4.8–12.7**	**11.0***	**6.5–15.9***	**Eurasia[a,d]**
***Anthacanthae* (8; CAM)**	**7.6**	**5.4–10.0**	**10.8***	**7.4–14.5***	**Africa[b,e,f]**
Anisophyllum	23.6	18.1–29.3	30.0	24.9–35.9	
***Monadenium* (3; CAM)**	**5.7***	**2.5–9.3***	**22.1**	**—**	**Africa[b,e,f]**
Euphorbia	14.0	10.5–17.8	20.5	—	
Other major clades					
***Helioscopia* V (2; C_3)**	**6.7**	**4.3–9.5**	**9.8***	**6.3–13.6***	**Eurasia[a,d]**
***Anisophyllum* subsection *Hypericifoliae* (6; C_4)**	**15.3***	**10.5–20.2***	**23.6**	**18.1–29.3**	**North America[g,h]**
***Tirucalli* + *Pervilleanae* (7; mostly CAM)**	**5.6***	**2.7–8.9***	**27.2**	**—**	**Madagascar[c]**
Goniostema + *Deuterocalli* + *Denisophorbia*	11.2	7.4–15.3	23.9	18.0–29.8	
***Goniostema* II + *Denisophorbia* (4; mostly CAM)**	**8.3**	**5.2–11.7**	**9.4***	**6.2–13.1***	**Madagascar[c]**
***Euphorbia* IX + X (1; CAM)**	**8.5**	**6.3–10.9**	**9.5***	**—**	**Africa[b,e,f]**

The eight clades with increased net diversification rates identified by the MEDUSA analysis are indicated in boldface type and numbered with Arabic numerals following Tables 2 and 4 and Figures 2 and 3. An asterisk is placed next to the dates that correspond to the shift position (crown or stem). Area of origin and photosynthetic pathway type typical for each these eight clades are also indicated. Superscript letters to the right of area of origin indicate references that document an expansion of dryland ecosystems in these areas from the mid-Miocene to the early Pliocene.

[a]Suc (1984). [b]Partridge (1993). [c]Wells (2003). [d]Guo et al. (2004). [e]Jacobs (2004). [f]Dupont et al. (2011). [g]Graham (2011). [h]Eronen et al. (2012).

A dash under stem age indicates that the node subtending the stem lineage of the given clade was not recovered with sufficient frequency to calculate its 95% highest posterior density (HPD) interval. Ages are in millions of years before present (Ma).

Table 2. Divergence times for CCM origins within *Euphorbia*.

CCM type and clade (or tip) of origin	Median crown age	95% HPD crown age	Median stem age	95% HPD stem age	Area of origin	Position of CCM origin relative to shift in *r*
C_4 (subgenus *Chamaesyce* only)						
Anisophyllum* subsection *Hypericifoliae	**15.3**	**10.5–20.2**	**23.6**	**18.1–29.3**	**North America**	**Before Shift 6 (crown of this clade)**
Strong CAM (all four subgeneric clades)						
Subgenus *Esula* (section *Aphyllis* only)						
E. mauritanica	Tip	Tip	3.5	1.7–5.6	Africa	No shift
E. schimperi	Tip	Tip	3.4	1.7–5.2	Africa	No shift
E. lateriflora	Tip	Tip	2.7	1.1–4.3	Africa	No shift
Subgenus *Athymalus*						
Balsamis: *E. larica*	Tip	Tip	6.7	3.0–10.5	SW Asia	No shift
§*Anthacanthae*: *E. heptagona* to *E. fimbriata*	**5.2**	**3.5–7.0**	**6.8**	**4.7–9.1**	**Africa**	**After Shift 8 (stem of *Anthacanthae*)**
****Anthacanthae*: *E. heptagona* + *E. pseudoglobosa***	**3.2**	**1.3–5.2**	**5.2**	**3.5–7.0**	**Africa**	**After Shift 8 (stem of *Anthacanthae*)**
****Anthacanthae*: *E. aggregata***	**Tip**	**Tip**	**1.2**	**0.4–2.3**	**Africa**	**After Shift 8 (stem of *Anthacanthae*)**
****Anthacanthae*: *E. jansenvillensis* to *E. fimbriata***	**2.2**	**1.3–3.2**	**3.6**	**2.3–5.0**	**Africa**	**After Shift 8 (stem of *Anthacanthae*)**
Anthacanthae*: *E. pedemontana* to *E. bergeri	**5.8**	**4.0–7.7**	**7.6**	**5.4–10.0**	**Africa**	**After Shift 8 (stem of *Anthacanthae*)**
Subgenus *Chamaesyce*						
Madagascar clade: *E. platyclada*	Tip	Tip	23.6	13.7–32.7	Madagascar	No shift
Articulofruticosae	7.1	2.1–12.9	34.3	—	Africa	No shift
Alectoroctonum: *E. ceroderma*	Tip	Tip	11.9	—	North America	No shift
Subgenus *Euphorbia*						
Tirucalli	3.2	**1.7–4.9**	**5.6**	**2.7–8.9**	**Madagascar**	**After Shift 7 (crown of *Pervilleanae* + *Tirucalli*)**
New World: *E. weberbaueri*	Tip	Tip	10.5	5.2–16.0	South America	No shift
New World: *E. lomelii*	Tip	Tip	6.5	2.7–10.4	North America	No shift
New World: *E. sipolisii*	Tip	Tip	12.8	7.1–18.2	South America	No shift
Deuterocalli: *E. alluaudii*	Tip	Tip	9.4	6.2–13.1	Madagascar	No shift
Goniostema*: *E. francoisii* to *E. decaryi	**3.7**	**1.9–5.7**	**5.9**	**3.5–8.6**	**Madagascar**	**After Shift 4 (stem of *Goniostema* II + *Denisophorbia*)**
Monadenium	**5.7**	**2.5–9.3**	**22.1**	**—**	**Africa**	**Before Shift 3 (crown of this clade)**
Euphorbia	**14.0**	**10.5–17.8**	**20.5**	**—**	**Africa**	**Before Shift 1 (stem of *Euphorbia* IX + X)**

Information based on ML ancestral state reconstructions using the set of 1000 197-tip chronograms (Figs. 2 and S4) and temporally interpreted using the results of the BEAST analysis. The ages given are for the optimizations using a two-rate model ($q_{01} >> q_{10}$). Transition rate values were set to the median parameter values from the ML BiSSE analysis (six-parameter model; Table 6), and the $\delta^{13}C$ values binned using a cutoff value of $-20‰$. Each CCM origin occurs along the stem lineage subtending the crown clade or tip species given below. CCM origins related to shifts in net diversification rates (*r*) identified by the MEDUSA analysis are indicated in boldface type. Shifts are numbered with Arabic numerals following Tables 1 and 4 and Figures 2 and 3. A dash under stem age indicates that the node subtending the stem lineage of a given clade was not recovered with sufficient frequency to calculate its 95% highest posterior density (HPD) interval. Ages are in millions of years before present (Ma). Alternative hypotheses of CAM origin for a clade within section *Anthacanthae* are indicated by § for single origin and asterisk (*) for multiple origin interpretations. Not shown is a possible common origin of CAM in sections *Euphorbia* and *Monadenium* because poor phylogenetic resolution precludes adequate ancestral state and dating estimation.

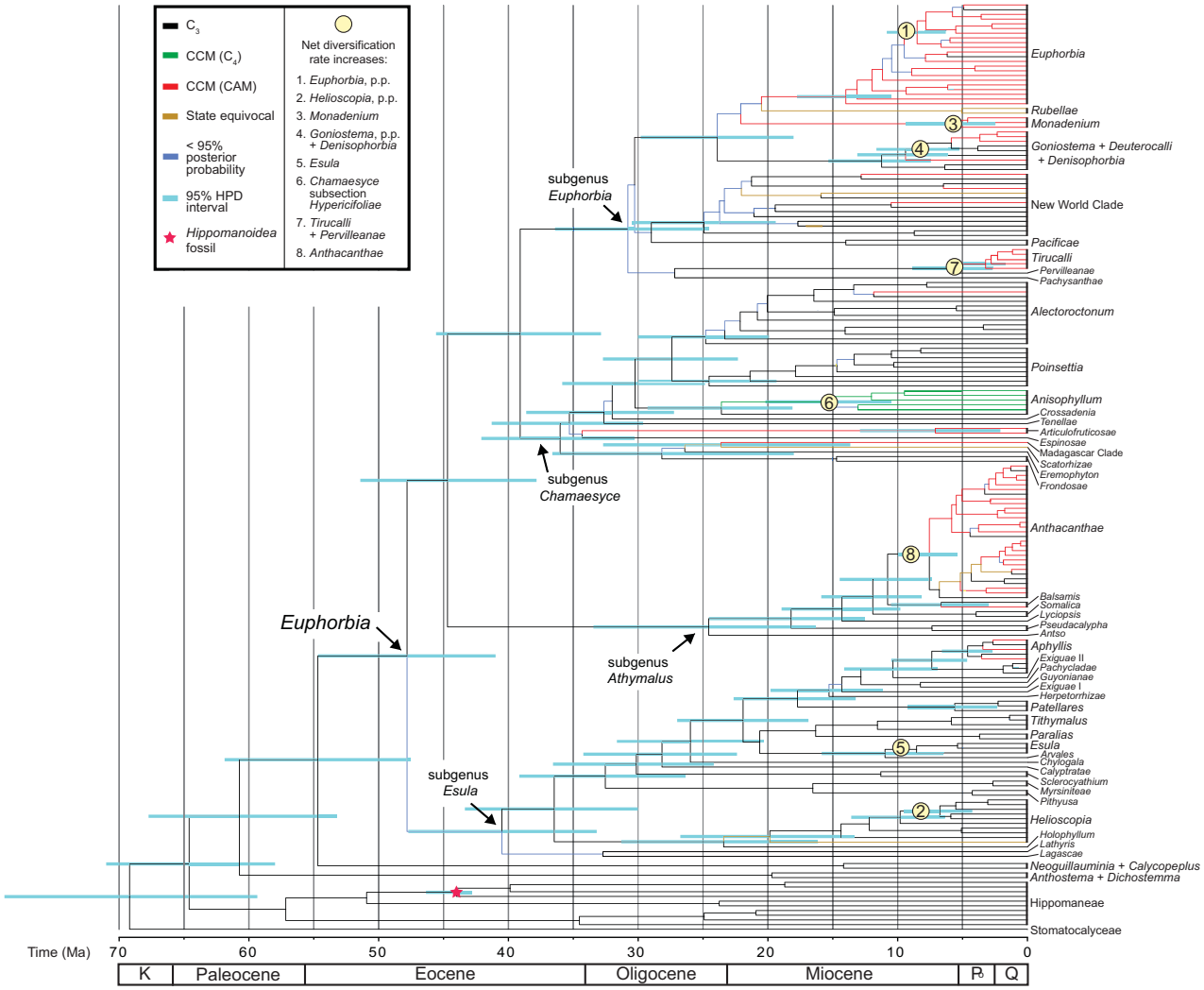

Figure 2. Dated chronogram (maximum clade credibility tree) inferred from the BEAST analysis of the 197-tip dataset of *Euphorbia* and outgroups. Tip labels within *Euphorbia* are names of sectional clades (see Table S4 for further information). Ancestral state reconstruction of photosynthetic system type: C_3-like, with atmospheric CO_2 predominantly fixed by RuBisCO, or CCM with CO_2 principally fixed by PEPC using a −20‰ cutoff of the $\delta^{13}C$ values under the two-rate transition model indicated by colored branches (see legend in figure and also Table 2). Lineages in which a significant shift in the net diversification rate (*r*) was modeled in >50% of the 1000 diversity trees in the MEDUSA analysis are mapped with numbered circles and further detailed in Table 4.

Table 3. Background net diversification rate (*r*) and tree model type for the root of the clade of Euphorbioideae and stem lineage of *Euphorbia* estimated using the MEDUSA method.

Lineage for background value of *r*	Mean value of *r*	Median value of *r*	Standard deviation of *r*	Tree model
Euphorbioideae	0.0764	0.0771	0.0131	Birth–death
Euphorbia	0.0796	0.0778	0.0159	Birth–death

Estimates are based upon an analysis of 1000 diversity trees. Values of *r* are interpreted as net speciation events per million years.

We interpret these two submodels as constituting a confidence set because Akaike weights, based on median ΔAIC values, indicate that they have a combined, conditional probability of ≈0.997. Similar to Beaulieu and Donoghue (2013), we noted an issue with correlated (and compensatory) speciation (λ) and extinction rates (μ) in the results of our ML BiSSE analyses, perhaps due to difficulties in estimating extinction rates from molecular phylogenetic information (Rabosky 2010), and we present estimates of these parameters as the net diversification rate ($r = \lambda - \mu$). Median values of *r* associated with strongly expressed CCM fixation (state

Table 4. Clades for which a significant shift in the net diversification rate (*r*) was modeled in >50% of 1000 diversity trees using the MEDUSA method.

Clade number	Clade membership, placement of shift in *r*, estimated species diversity, and typical photosynthetic pathway type	Percentage of trees in which shift was modeled	Mean value of shift in *r*	Median value of shift in *r*	Standard deviation of shift value	Maximum value of shift in *r*	Minimum value of shift in *r*	Tree model
1	*Euphorbia* IX + X, stem; 297 spp.; CAM	96.0%	0.4356	0.4295	0.1017	0.7954	0.2257	Yule
2	*Helioscopia* V, stem; 107 spp.; C_3	91.3%	0.4104	0.4023	0.1009	1.0367	0.1680	Yule
3	*Monadenium*, crown; 90 spp.; CAM	81.9%	0.6560	0.6245	0.2059	1.4830	0.2104	Yule
4	*Goniostema* II + *Denisophorbia*, stem; 83 spp.; mostly weak to strong CAM	78.7%	0.3859	0.3781	0.0935	0.7424	0.1418	Yule
5	*Esula*, stem; 96 spp.; C_3	78.1%	0.3615	0.3502	0.1012	0.8597	0.1566	Yule
6	*Anisophyllum* subsection *Hypericifoliae*, crown; 360 spp.; C_4	70.8%	0.3162	0.3137	0.1111	0.7233	−0.0802	Yule
7	*Tirucalli* + *Pervilleanae*, crown; 32 spp.; mostly CAM	51.8%	0.4989	0.4777	0.1512	1.2936	0.1614	Yule
8	*Anthacanthae*, stem; 166 spp.; mostly CAM	50.2%	0.4961	0.4911	0.0881	0.7837	0.1722	Yule

Clade numbers in Arabic numerals correspond to those of mapped shifts in Figures 2 and 3 and clades in boldface type in Tables 1 and 2. Shift values are relative to those of a background value of *r* (see Table 3). Values of *r* are interpreted as net speciation events per million years.

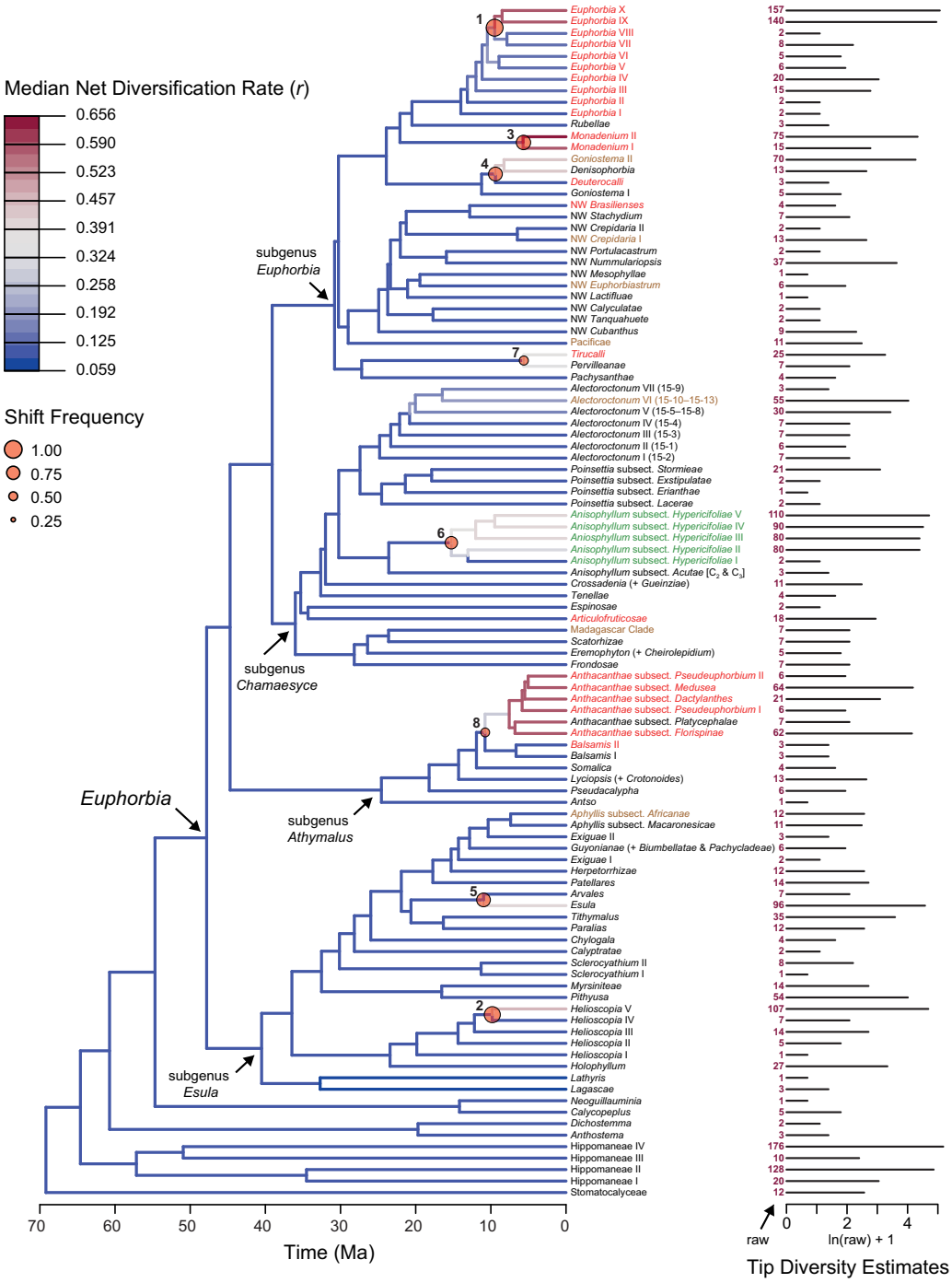

Figure 3. Plot of a diversity tree chronogram obtained by pruning the maximum clade credibility tree inferred from the BEAST analysis to 104 tips. All sectional clades recognized within *Euphorbia* are included here, except the monotypic section *Szovitsiae* of subgenus *Esula*. Raw tip diversity values are listed in purple Arabic numerals to the left of the bars displaying log-transformed tip diversities. Branches of the diversity tree are shaded according the corresponding median value of the net diversification rate (*r*) obtained from MEDUSA optimizations across 1000 diversity trees (see legend). Plotted rate shifts were present in >50% of the diversity trees (see legend). Black Arabic numerals next to the plotted rate shifts correspond with those in Fig. 2 and Tables 1, 2, and 4. Different font colors for the tip clade names indicate the characteristic photosynthetic pathway type for the lineage: C_3 = black; C_4 = green; predominantly strong CAM = red; strong CAM present in some species = brown. The "NW" preceding several sectional names in subgenus *Euphorbia* indicates membership within the New World clade, as shown in Figure 2. Arabic numerals in parentheses next to the seven subclades of section *Alectoroctonum* correspond with subclades recognized in Yang et al. (2012; see their Fig. 3b). See Tables 3 and 4 for further information on values of *r* obtained and Table S4 for further information on tip labels and diversities.

Table 5. Median likelihood statistics ± estimated interquartile range from analyses of the 1000 diversity trees for the eight BiSSE submodels, sorted from best-fitting model at the top (confidence set indicated in boldface type) to the worst at the bottom.

Model specification						
Speciation rate	Extinction rate	Transition rate	Number of parameters	Log likelihood	ΔAIC	Akaike weight
Free	**Free**	**Free**	**6**	**−826.88 ± 5.73**	**0**	**0.666**
Free	**Free**	**Constrained**	**5**	**−828.58 ± 5.74**	**1.43 ± 0.89**	**0.331**
Free	Constrained	Constrained	4	−834.79 ± 6.05	12.05 ± 4.21	1.80×10^{-3}
Free	Constrained	Free	5	−834.20 ± 5.95	12.78 ± 3.99	1.12×10^{-3}
Constrained	Free	Free	5	−838.28 ± 6.12	20.71 ± 5.48	2.03×10^{-5}
Constrained	Free	Constrained	4	−839.94 ± 6.24	22.07 ± 5.66	1.04×10^{-5}
Constrained	Constrained	Constrained	3	−867.30 ± 5.85	75.41 ± 6.83	3.74×10^{-17}
Constrained	Constrained	Free	4	−867.27 ± 5.84	77.29 ± 6.86	1.42×10^{-17}

Model fit is determined by ΔAIC, which is the AIC value relative to that of the best-fitting model (ΔAIC = 0). The weight of evidence for each model from the set of models used is given by the Akaike weight. Parameter values for the BiSSE submodels are given in Table 6.

Table 6. Median net diversification (*r*) and character state transition rates ± estimated interquartile range from analyses of the 1000 diversity trees for the eight BiSSE submodels, sorted from best-fitting model at the top (confidence set indicated in boldface type) to the worst at the bottom, in parallel with model ranking given in Table 5.

Model specification				Net diversification rate		Transition rate	
Speciation rate	Extinction rate	Transition rate	Number of parameters	r_0 (C_3)	r_1 (CCM)	q_{01} ($C_3 \rightarrow$ CCM)	q_{10} (CCM $\rightarrow C_3$)
Free	**Free**	**Free**	**6**	**0.062 ± 0.012**	**0.177 ± 0.045**	**0.009 ± 0.003**	**0.002 ± 0.001**
Free	**Free**	**Constrained**	**5**	**0.065 ± 0.010**	**0.218 ± 0.048**	**0.005 ± 0.001**	**0.005 ± 0.001**
Free	Constrained	Constrained	4	0.062 ± 0.011	0.353 ± 0.068	0.002 ± 0.000	0.002 ± 0.000
Free	Constrained	Free	5	0.061 ± 0.011	0.353 ± 0.067	0.002 ± 0.000	0.004 ± 0.001
Constrained	Free	Free	5	0.057 ± 0.004	0.387 ± 0.090	0.002 ± 0.000	0.005 ± 0.001
Constrained	Free	Constrained	4	0.057 ± 0.001	0.379 ± 0.086	0.002 ± 0.000	0.002 ± 0.000
Constrained	Constrained	Constrained	3	0.053 ± 0.008	0.053 ± 0.008	0.005 ± 0.001	0.005 ± 0.001
Constrained	Constrained	Free	4	0.053 ± 0.008	0.053 ± 0.008	0.005 ± 0.001	0.005 ± 0.001

1) were about three times greater than those associated with C_3-like carbon fixation (state 0) for the two submodels of the confidence set (Tables 5 and 6). Estimates of *r* from Bayesian analyses of the confidence set submodels corroborate the ML results (Fig. 4). Estimates of the values of each of the BiSSE model parameters from these analyses also suggest that trait-based differences in *r* are due to relatively lower extinction rates in CCM lineages, with CCM and C_3 speciation rates being about equal (Fig. S7).

Discussion

Rapid regional aridification in the low-CO_2 world of the mid- to late-Miocene would have likely changed the abiotic parameters of areas into which dryland ecosystems expanded. Heightened environmental stress from increasingly limited precipitation and seasonal drought would have introduced a correspondingly strong mode of directional selection favoring increased drought tolerance or avoidance. Responses by affected biota were likely complex, involving range shifts, local extirpation, and species extinction, in addition to in situ persistence coupled with local adaptation through phenotypic change (Davis et al. 2005). Evidence of the latter is supported from studies of arid-adapted plants, which demonstrate accelerated net diversification in some CCM lineages, such as cacti and iceplants, approximately coinciding with the Miocene expansion of arid ecosystems (Verboom et al. 2009; Arakaki et al. 2011; Valente et al. 2014). *Euphorbia* is also a rich system for understanding plant evolution and diversification in arid ecosystems because *Euphorbia* lineages were present in four geographically distinct areas in which these ecosystems progressively expanded in the mid-Miocene (i.e., southern and eastern Africa, Madagascar, southwestern North America, and southern Eurasia; Table 1 [biogeographic hypotheses from: Zimmerman et al. 2010; Yang and Berry 2011; Yang et al. 2012; Dorsey et al. 2013; Peirson et al. 2013; Riina et al. 2013; temporally interpreted using our Figs. 2 and S2]). These

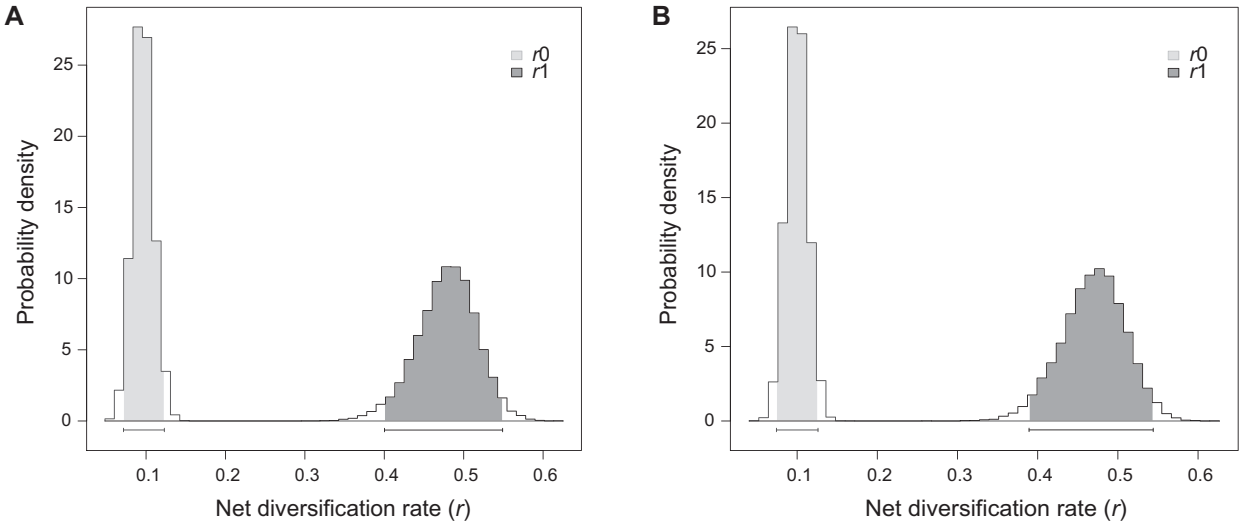

Figure 4. Density plots of posterior probability distributions for values of the net diversification rate r ($r = \lambda - \mu$) for *Euphorbia* and outgroups. These values were estimated from a Bayesian MCMC analysis of the confidence set of BiSSE submodels (see Tables 5 and 6) using a diversity tree based on the maximum clade credibility tree from the BEAST analysis. The full distributions are indicated within the outline of each curve; the shaded area within each curve is the 95% HPD interval, which is further indicated by the bar beneath the curve. (A) Distribution of estimated values of r_0 (C_3) and r_1 (CCM: C_4 and CAM) from the full, six-parameter BiSSE submodel. (B) Distribution of estimated values of r_0 (C_3) and r_1 (CCM: C_4 and CAM) from the five-parameter BiSSE submodel in which forward and reverse transition rates are constrained ($q_{01} = q_{10}$).

phylogenetically and geographically independent replicates in our results indicate that both the timing of CCM physiology origins and lineage-specific shifts in net diversification rate (r) largely coincide with the advent of novel ecological opportunity resulting from expanding aridification in the Miocene through the Pliocene.

CCM ORIGINS AND INCREASED SPECIES DIVERSIFICATION ARE BROADLY CONTEMPORANOUS IN *EUPHORBIA*

Euphorbia is the only known subclade of Euphorbiaceae to exhibit CCMs. Our ancestral state reconstructions, coupled with divergence dating information, indicate that strong CCM expression evolved 17–22 times within the four subgeneric clades. All but one of these transitions are to strong CAM expression, and they occurred mostly from the mid-Miocene through the Pliocene (Table 2; Figs. 2, S3, S4). The numerous strong CAM origins are replicated within each of the subgeneric clades, and, likewise, geographically replicated (Table 2). The C_4 pathway has a single, North American origin within *Euphorbia* along the stem lineage of section *Anisophyllum* subsection *Hypericifoliae* (Yang and Berry 2011). This clade is the largest C_4 eudicot clade (365 spp.; Yang et al. 2012) and, perhaps, the oldest of the ~36 C_4 origins in eudicots, given its mid-Oligocene to early-Miocene stem age and early- to mid-Miocene crown age (Table 2; Christin et al. 2011; Sage et al. 2011a).

Strong CAM expression in *Euphorbia* is characteristic of organs exhibiting succulence—typically stems (Fig. 1G; Webster et al. 1975; Dorsey 2013)—that sustain photosynthetic function through repeated episodes of seasonal drought. It is clear that evolutionary access to strong CAM expression in *Euphorbia* is much greater than the ability of CAM lineages to successfully disperse away from their continent of origin (the major exception being a dispersal event to southeast Asia in section *Euphorbia*; Bruyns et al. 2011; Dorsey 2013). Hence, the continental distribution of most strong CAM lineages in *Euphorbia* is a function of their evolution in situ. If some degree of phenotypic plasticity with regard to nascent CAM expression was ancestral in *Euphorbia*—as its multiple origins within each of the four subgeneric clades might suggest—then CAM origins may ultimately be linked to its inducibility as a stress response to scavenge respiratory CO_2 during periods of acute water stress when stomata are closed (Ehleringer and Monson 1993; West-Eberhard 2003). The apparent ease of evolutionary transitions to strong CAM expression in *Euphorbia* was likely enabled by preexisting facultative modes of CAM, as has been hypothesized in other angiosperm clades (Dodd et al. 2002; Edwards and Ogburn 2012). Facultative CAM expression does occur in *Euphorbia*, although knowledge of its overall distribution remains limited (see Figs. S4 and S5).

In terrestrial plants with facultative CAM, CAM expression is strongly environmentally mediated, typically in response to drought stress (Winter and Holtum 2011). The inherent plasticity of CAM expression is, correspondingly, thought to enable a flexible evolutionary trajectory that parallels adaptive evolution into a diversity of arid niches (Lüttge 2004, 2007), including obligate

CAM expression in particularly arid environments (Dodd et al. 2002). In our results, the narrow time-frame bracketing most of these transitions in *Euphorbia* is coincident with the mid-Miocene/Pliocene expansion of arid ecosystems. The increased availability, and perhaps diversity, of arid niche space during this period may have provided greater opportunity for CAM specialization, facilitating the numerous strong CAM origins in this clade.

Perhaps similar to the few oldest transitions to CAM, the transition to a fully optimized C_4 pathway in section *Anisophyllum* subsection *Hypericifoliae* likely predates mid-Miocene aridification (Table 2), suggesting that its environmental drivers were distinct from the expansion of dryland ecosystems. As Spriggs et al. (2014) suggest for C_4 grasses, pockets of open, seasonally dry habitat were likely present at mid-latitudes in the more mesic environment of the early- to mid-Miocene, where C_4 plants would have had an adaptive advantage. Members of section *Anisophyllum* may have occupied such habitats in southwestern North America as far back as the early Oligocene, where the origin of the C_2 pathway (a C_3-C_4 intermediate), present in two of the three species of subsection *Acutae*, sister to subsection *Hypericifoliae* (Table 1; Sage et al. 2011b; Yang and Berry 2011), would have enabled scavenging of photorespiratory CO_2 in the newly CO_2-impoverished atmosphere of this period. Section *Anisophyllum* is the only ancestrally herbaceous *Euphorbia* clade in which CCMs evolved; CAM *Euphorbia* lineages were ancestrally woody (Horn et al. 2012). We hypothesize that this was an important factor in establishing an evolutionary trajectory toward the unique C_4 origin within the genus.

The results of our MEDUSA analyses also provide strong evidence that eight exceptional bursts of diversification in *Euphorbia* are clustered within a narrow time frame from the Miocene through the Pliocene (15.3–5.6 Ma; 20.2–2.5 Ma with 95% HPD; Table 1; Fig. 2). Our estimates of the background values of *r* for Euphorbioideae are comparable to those of major lineages of flowering plants (Table 3; Magallón and Castillo 2009), but the values of *r* we obtained for these eight *Euphorbia* lineages (Table 4) are substantially higher and comparable with some well-known examples of explosive angiosperm radiations (Baldwin and Sanderson 1998). These eight *Euphorbia* radiations occur in the four areas in which dryland ecosystems expanded in the mid-Miocene/Pliocene (Table 1), and, therefore, experienced similar ecological opportunity in these distinct regions. Six of the eight lineages associated with increases in *r* predominantly contain species with CCMs and include ~51% of all *Euphorbia* species. CCMs (both CAM and C_4) evolved prior to three rate shifts (Table 1: 1, 3, 6), with a transition from C_3 to CCM occurring along the stem lineage antecedent to a rate shift at the crown in two of these clades, strongly supporting the idea that CCMs can be a key innovation. CAM originated 5.7–0 Ma (13.2–0 Ma with 95% HPD) after the three other shifts (4, 7, 8). Here, new arid ecological opportunity appears to have initially promoted a diversity of adaptive strategies (especially shift 4; see Evans et al. 2014), possibly including weak or facultative modes of CAM (weak CAM in *E. milii*, Herrera 2013), with the transition(s) to strong CAM expression the most successful of these in terms of current species diversity. The remaining two lineages not associated with CCMs are both predominantly leafy, herbaceous clades within subgenus *Esula* that occur in temperate zones of Eurasia.

CCMs LINKED TO INCRESASED NET DIVERSIFICATION RATES IN *EUPHORBIA*: A CASE FOR SPECIES SELECTION?

Two lines of evolutionary evidence from our results support the idea that the evolution of strong CCM expression in *Euphorbia* is a key innovation in relation to the key opportunity provided by climate change. As just argued, a synthesis of the results of our ancestral state reconstructions and MEDUSA analysis is congruent with this hypothesis. The results of our BiSSE analyses additionally support the idea that CCMs are a key innovation. The confidence set contains two models in which speciation and extinction rates associated with CCM type are distinct, with values of *r* associated with CCM lineages ~3× greater that C_3 lineages (Table 6; Fig. 4). In this way, our results reflect those of recent studies that demonstrated a link between replicate CAM origins and increased *r* in bromeliads (Silvestro et al. 2014) and replicate C_4 origins and increased *r* in grasses (Bouchenak-Khelladi et al. 2014; Spriggs et al. 2014). Collectively, these results strongly suggest CCMs promote increases in *r*.

If this is true, then what explains the disparate diversification histories among stem succulent CAM lineages in *Euphorbia*? Unexceptional net diversification in the four, New World CAM succulent lineages may be related to competition from cacti, whose origins predate those of the New World *Euphorbia* CAM lineages by at least 10 Ma (Table 2; Arakaki et al. 2011). However, in CAM lineages from Africa and Madagascar, a correlation between shoot architecture and inflorescence position is potentially important to explaining differences in diversification histories. Horn et al. (2012) hypothesized that irreversible transitions from terminal to lateral inflorescences in *Euphorbia* xerophytes may enhance the survivorship of mature plants through a release from biomechanical and anatomical limitations. Correspondingly, the five bursts in net diversification associated with Old World CAM clades identified in the MEDUSA analysis (Figs. 2 and 3; Tables 1, 2, and 4) are confined to lineages in which the transition to lateral inflorescences occurred, whereas the Old World CAM lineages characterized by uniformly terminal inflorescences experienced unexceptional net diversification that is explicable by background rates. The weight of evidence suggests that although the relationship between CCM origins and exceptional

lineage diversification may indeed be a causal one in *Euphorbia*, it is likely also contingent upon other lineage-specific factors (Donoghue 2005).

Nevertheless, how can CCMs increase net species diversification? The fitness advantages conferred by CCMs in warm, water-limited, contemporary ecosystems are well known, but these benefits are typically conceptualized as enhancing survivorship of mature individuals. Yet our results provide compelling evidence to suggest that CCMs confer fitness advantages that are emergent at the species level in *Euphorbia*. The advantages to survivorship and differential reproductive success conferred by CCMs at the level of individual organisms may cascade upward to promote increased *r*, thus mediating species selection in the broad sense (Gould 2002; see also, Vrba 1984). We suggest two hypotheses, which need not be mutually exclusive, that explain our results in the context of species selection (Rabosky and McCune 2010).

The hypothesis most readily supported by our results is that CCM lineages have lower extinction rates relative to C_3 lineages in *Euphorbia*. In the results of our MEDUSA analysis, each of the eight lineages in which increases in *r* were frequently recovered is also accompanied by a change in tree model type from birth–death to pure birth (Yule model; Table 4), indicating that a model without extinction better fits the overall observed data for these lineages. This does not exclude the possibility that extinction occurred but does suggest that decreased extinction rates are key to explaining increases in *r*. The results of the Bayesian analysis of parameter values of the two BiSSE submodels in our confidence set further emphasize this point, indicating that although speciation rates for CCM and C_3 lineages are nearly equivalent, extinction rates of CCM lineages are generally lower than those of C_3 lineages (Fig. S7).

How might CCMs lower extinction rates? In arid and semiarid ecosystems, where more than a decade may pass between growing seasons that can sustain rainfall adequate to promote establishment (Jordan and Nobel 1979), plants are perhaps most vulnerable to the effects of drought during seedling and juvenile phases of growth. Because of this, a very low percentage of seedlings survive to maturity. In lineages such as *Euphorbia* that have a sizeable proportion of finely adapted endemic species with few populations, these endemics will be inherently at risk of extinction from the combined effects of demographic stochasticity, genetic drift, and environmental variation, which are thought to promote an extinction vortex in small populations (Gilpin and Soulé 1986). Adaptive traits that might increase WUE in juveniles or enhance fecundity may, therefore, have significantly increased the chance of recruitment of enough individuals to sustain population sizes large enough to be robust to these effects. Experimental studies comparing the survivorship of seedling C_3 and CCM *Euphorbia* species under drought conditions are lacking. However, with respect to CAM, the results of such studies in other lineages support our idea that CAM confers high WUE in seedlings (Hernández-González and Villarreal 2007), which can translate into markedly increased drought tolerance compared with seedlings of sympatric C_3 species (Esler and Phillips 1994). The coupling of form and C_4 physiology in section *Anisophyllum* likely facilitates high rate of seed production per unit time (Horn et al. 2012), in addition to facilitating remarkably short generation times such that multiple, overlapping generations can be established within a growing season in the many annual species of this clade (Suzuki and Teranishi 2005).

A second hypothesis to explain how CCMs might increase net diversification rates is that they may increase speciation rates. The potential capability of CCMs in *Euphorbia* to enhance seedling survivorship and establishment of populations in arid ecosystems suggests a mechanism that might have facilitated ecological release and range expansion into emerging dryland ecosystems (Yoder et al. 2010). In addition, *Euphorbia* seeds are chiefly ant dispersed (following ballistic capsule dehiscence), a syndrome that strongly limits dispersal distances and promotes geographic isolation (Lengyel et al. 2009). Generally limited dispersal, coupled with the possible benefits to establishment that CCMs confer, may have increased the rate of formation of peripheral isolate populations subsequent to rare seed dispersal events over longer distances, which, in turn, may have promoted increased speciation rates in some CCM *Euphorbia* lineages. Our results do not unequivocally indicate that CCMs promoted increased speciation rates in *Euphorbia*, but the high values of *r* estimated for several of the CCM lineages in our MEDUSA analysis (Table 4) are consistent with a combination of decreased extinction rates and increased speciation rates. If CCMs did promote higher speciation rates in this manner, then the capacity for rapid phenotypic change within *Euphorbia* was likely critical to enabling differentiation and local adaptation among such populations, engendering this spectacular angiosperm radiation.

ACKNOWLEDGMENTS

The authors thank J. W. Brown, R. FitzJohn, G. Hunt, M. Kweskin, and G. Slater for advice on the analyses. C. France of the Smithsonian Museum Conservation Institute conducted the stable isotope analyses. A. Tangerini and S. Yankowski assisted in preparing Figure 1. The National Science Foundation (PBI grant DEB-0616533 and AToL grant DEB-0622764) and the Smithsonian Institution supported this study.

DATA ARCHIVING

The doi for our data is 10.5061/dryad.sb1j1.

LITERATURE CITED

Ackerly, D. D. 2009. Evolution, origin and age of lineages in the Californian and Mediterranean floras. J. Biogeogr. 36:1221–1233.

Akaike, H. 1974. A new look at the statistical model identification. IEEE Trans. Automat. Contr. 19:716–723.

Alfaro, M. E., F. Santini, C. Brock, H. Alamillo, A. Dornburg, D. L. Rabosky, G. Carnevale, and L. J. Harmon. 2009. Nine exceptional radiations plus high turnover explain species diversity in jawed vertebrates. Proc. Natl. Acad. Sci. USA 106:13410–13414.

Alvarado-Cárdenas, L. O., E. Martínez-Meyer, T. P. Feria, L. E. Eguiarte, H. M. Hernández, G. Midgley, and M. E. Olson. 2013. To converge or not to converge in environmental space: testing for similar environments between analogous succulent plants of North America and Africa. Ann. Bot. 111:1125–1138.

Anderson, C. J., A. Channing, and A. B. Zamuner. 2009. Life, death and fossilization on Gran Canaria—implications for Macaronesian biogeography and molecular dating. J. Biogeogr. 36:2189–2201.

Arakaki, M., P.-A. Christin, R. Nyffeler, A. Lendel, U. Eggli, R. M. Ogburn, E. Spriggs, M. J. Moore, and E. J. Edwards. 2011. Contemporaneous and recent radiations of the world's major succulent plant lineages. Proc. Natl. Acad. Sci. USA 108:8379–8384.

Baldwin, B. G., and M. J. Sanderson. 1998. Age and rate of diversification of the Hawaiian silversword alliance (Compositae). Proc. Natl. Acad. Sci. USA 95:9402–9406.

Beaulieu, J. M., and M. J. Donoghue. 2013. Fruit evolution and diversification in campanulid angiosperms. Evolution 67:3132–3144.

Beerling, D. J., and D. L. Royer. 2011. Convergent Cenozoic CO_2 history. Nat. Geosci. 4:418–420.

Bender, M. M. 1971. Variations in the $^{13}C/^{12}C$ ratios of plants in relation to the pathway of photosynthetic carbon dioxide fixation. Phytochemistry 10:1239–1244.

Bender, M. M., I. Rouhani, H. M. Vines, and C. C. Black Jr. 1973. $^{13}C/^{12}C$ ratio changes in crassulacean acid metabolism plants. Plant Physiol. 52:427–430.

Borland, A. M., V. A. Barrera Zambrano, J. Ceusters, and K. Shorrock. 2011. The photosynthetic plasticity of crassulacean acid metabolism: an evolutionary innovation for sustainable productivity in a changing world. New Phytol. 191:619–633.

Bouchenak-Khelladi, Y., J. A. Slingsby, G. A. Verboom, and W. J. Bond. 2014. Diversification of C_4 grasses (Poaceae) does not coincide with their ecological dominance. Am. J. Bot. 101:300–307.

Bruyns, P. V., C. Klak, and P. Hanáček. 2011. Age and diversity in Old World succulent species of *Euphorbia* (Euphorbiaceae). Taxon 60:1717–1733.

Burnham, K. P., and D. R. Anderson. 2002. Model selection and inference: a practical information-theoretic approach. 2nd ed. Springer Verlag, New York, NY.

Bytebier, B., A. Antonelli, D. U. Bellstedt, and H. P. Linder. 2011. Estimating the age of fire in the Cape Flora of South Africa from an orchid phylogeny. Proc. R. Soc. Lond. B 278:188–195.

Cerling, T. E., Y. Wang, and J. Quade. 1993. Expansion of C_4 ecosystems as an indicator of global ecological change in the late Miocene. Nature 361:344–345.

Cerling, T. E., J. M. Harris, B. J. MacFadden, M. G. Leakey, J. Quade, V. Eisenmann, and J. R. Ehleringer. 1997. Global vegetation change through the Miocene/Pliocene boundary. Nature 389:153–158.

Christin, P.-A., C. P. Osborne, R. F. Sage, M. Arakaki, and E. J. Edwards. 2011. C_4 eudicots are not younger than C_4 monocots. J. Exp. Bot. 62:3171–3181.

Christin, P.-A., M. Arakaki, C. P. Osborne, A. Bräutigam, R. F. Sage, J. M. Hibberd, S. Kelly, S. Covshoff, G. Ka-Shu Wong, L. Hancock, et al. 2014a. Shared origins of a key enzyme during the evolution of C_4 and CAM metabolism. J. Exp. Bot. 65:3609–3621.

Christin, P.-A., E. Spriggs, C. P. Osborne, C. A. E. Strömberg, N. Salamin, and E. J. Edwards. 2014b. Molecular dating, evolutionary rates, and the age of the grasses. Syst. Biol. 63:153–165.

Crayn, D. M., K. Winter, and A. C. Smith. 2004. Multiple origins of crassulacean acid metabolism and the epiphytic habit in the Neotropical family Bromeliaceae. Proc. Natl. Acad. Sci. USA 101:3703–3708.

Crepet, W. L., and C. P. Daghlian. 1982. Euphorbioid inflorescences from the Middle Eocene Clairborne formation. Am. J. Bot. 69:258–266.

Cushman, J. C. 2001. Crassulacean acid metabolism. A plastic photosynthetic adaptation to arid environments. Plant Physiol. 127:1439–1448.

Davis, M. B., R. G. Shaw, and J. R. Etterson. 2005. Evolutionary responses to changing climate. Ecology 86:1704–1714.

de Queiroz, A. 2002. Contingent predictability in evolution: key traits and diversification. Syst. Biol. 51:917–929.

Dodd, A. N., A. M. Borland, R. P. Haslam, H. Griffiths, and K. Maxwell. 2002. Crassulacean acid metabolism: plastic, fantastic. J. Exp. Bot. 53:569–580.

Donoghue, M. J. 2005. Key innovations, convergence, and success: macroevolutionary lessons from plant phylogeny. Paleobiology 31:77–93.

Dorsey, B. L. 2013. Phylogenetics and morphological evolution of *Euphorbia* subgenus *Euphorbia*. Ph.D. dissertation, University of Michigan, Ann Arbor, MI.

Dorsey, B. L., T. Haevermans, X. Aubriot, J. J. Morawetz, R. Riina, V. W. Steinmann, and P. E. Berry. 2013. Phylogenetics, morphological evolution, and classification of *Euphorbia* subgenus *Euphorbia*. Taxon 62:291–315.

Drummond, A. J., S. W. Y. Ho, M. J. Phillips, and A. Rambaut. 2006. Relaxed phylogenetics and dating with confidence. PLoS Biol. 4:699–710.

Drummond, A. J., M. A. Suchard, D. Xie, and A. Rambaud. 2012. Bayesian phylogenetics with BEAUti and the BEAST 1.7. Mol. Biol. Evol. 29:1969–1973.

Dupont, L. M., H. P. Linder, F. Rommerskirchen, and E. Schefuß. 2011. Climate-driven rampant speciation of the Cape Flora. J. Biogeogr. 38:1059–1068.

Edwards, E. J., and R. M. Ogburn. 2012. Angiosperm responses to a low-CO_2 world: CAM and C_4 photosynthesis as parallel evolutionary trajectories. Int. J. Plant Sci. 173:724–733.

Edwards, E. J., and S. A. Smith. 2010. Phylogenetic analyses reveal the shady history of C_4 grasses. Proc. Natl. Acad. Sci. USA 107:2532–2537.

Ehleringer, J. R., and R. K. Monson. 1993. Evolutionary and ecological aspects of photosynthetic pathway variation. Annu. Rev. Ecol. Evol. Syst. 24:411–439.

Eronen, J. T., M. Fortelius, A. Micheels, F. T. Portmann, K. Puolamäki, and C. M. Janis. 2012. Neogene aridification of the Northern Hemisphere. Geology 40:823–826.

Esler, K. J., and N. Phillips. 1994. Experimental effects of water-stress on semiarid karoo seedlings: implications for field seedling survivorship. J. Arid Environ. 26:325–337.

Esser, H.-J., P. E. Berry, and R. Riina. 2009. EuphORBia: a global inventory of the spurges. Blumea 54:11–12.

Evans, M., X. Aubriot, D. Hearn, M. Lanciaux, S. Lavergne, C. Cruaud, P. P. Lowry, and T. Haevermans. 2014. Insights on the evolution of plant succulence from a remarkable radiation in Madagascar (*Euphorbia*). Syst. Biol. 63:698–711.

Farquhar, G. D., J. R. Ehleringer, and K. T. Hubick. 1989. Carbon isotope discrimination and photosynthesis. Annu. Rev. Plant Physiol. 40:503–537.

FitzJohn, R. G. 2012. Diversitree: comparative phylogenetic analyses of diversification in R. Methods Ecol. Evol. 3:1084–1092.

FitzJohn, R. G., W. P. Maddison, and S. P. Otto. 2009. Estimating trait-dependent speciation and extinction rates from incompletely resolved phylogenies. Syst. Biol. 58:595–611.

Friis, E. M., and W. L. Crepet. 1987. Time and appearance of floral features. Pp. 145–180 *in* E. M. Friis, W. G. Chaloner, and P. R. Crane, eds. The origins of angiosperms and their biological consequences. Cambridge Univ. Press, New York, NY.

Gilpin, M. E., and M. E. Soulé. 1986. Minimum viable populations: processes of species extinction. Pp. 19–34 *in* M. E. Soulé, ed. Conservation biology: the science of scarcity and diversity. Sinauer Associates, Sunderland, MA.

Givnish, T. J., M. H. J. Barfuss, B. Van Ee, R. Riina, K. Schulte, R. Horres, P. A. Gonsiska, R. S. Jabaily, D. M. Crayn, et al. 2014. Adaptive radiation, correlated and contingent evolution, and net species diversification in Bromeliaceae. Mol. Phylogenet. Evol. 71:55–78.

Goldberg, E. E., and B. Igić. 2008. On phylogenetic tests of irreversible evolution. Evolution 62:2727–2741.

Good-Avila, S. V., V. Souza, B. S. Gaut, and L. E. Eguiarte. 2006. Timing and rate of speciation in *Agave* (Agavaceae). Proc. Natl. Acad. Sci. USA 103:9124–9129.

Gould, S. J. 2002. The structure of evolutionary theory. Belknap Press, Cambridge, MA.

Graham, A. 2011. The age and diversification of terrestrial New World ecosystems through Cretaceous and Cenozoic time. Am. J. Bot. 98:336–351.

Guo, Z., S. Peng, Q. Hao, P. E. Biscayne, Z. An, and T. Liu. 2004. Late Miocene–Pliocene development of Asian aridification as recorded in the Red-Earth Formation in northern China. Global Planet. Change 41:135–145.

Gutierrez, M., V. E. Gracen, and G. E. Edwards. 1974. Biochemical and cytological relationships in C_4 plants. Planta 119:279–300.

Hernández-Gonzáles, O., and O. B. Villarreal. 2007. Crassulacean acid metabolism photosynthesis in columnar cactus seedlings during ontogeny: the effect of light on nocturnal acidity accumulation and chlorophyll fluorescence. Am. J. Bot. 94:1344–1351.

Hernández-Hernández, T., J. W. Brown, B. O. Schlumpberger, L. E. Eguiarte, and S. Magallón. 2014. Beyond aridification: multiple explanations for the elevated diversification of cacti in the New World Succulent Biome. New Phytol. 202:1382–1397.

Herrera, A. 2009. Crassulacean acid metabolism and fitness under water deficit stress: if not for carbon gain, what is facultative CAM good for? Ann. Bot. 103:645–653.

———. 2013. Crassulacean acid metabolism-cycling in *Euphorbia milii*. AoB Plants 5:plt014. doi:10.1093/aobpla/plt014

Horn, J. W., B. W. van Ee, J. J. Morawetz, R. Riina, V. W. Steinmann, P. E. Berry, and K. J. Wurdack. 2012. Phylogenetics and evolution of major structural characters in the giant genus *Euphorbia* (Euphorbiaceae). Mol. Phylogenet. Evol. 63:305–326.

Jacobs, B. F. 2004. Paleobotanical studies from tropical Africa: relevance to the evolution of forest, woodland and savannah biomes. Philos. Trans. R. Soc. Lond. B 359:1573–1583.

Jordan, P. W., and P. S. Nobel. 1979. Infrequent establishment of seedlings of *Agave deserti* (Agavaceae) in the northwestern Sonoran Desert. Am. J. Bot. 66:1079–1084.

Kadereit, G., D. Ackerly, and M. D. Pirie. 2012. A broader model for C_4 photosynthesis evolution in plants inferred from the goosefoot family (Chenopodiaceae s.s.). Proc. R. Soc. Lond. B 279:3304–3311.

Keeley, J. E., and P. W. Rundell. 2003. Evolution of CAM and C_4 carbon-concentrating mechanisms. Int. J. Plant Sci. 164:S55–S77.

Keeling, C. D., W. G. Mook, and P. P. Tans. 1979. Recent trends in the $^{13}C/^{12}C$ ratio of atmospheric carbon dioxide. Nature 277:121–123.

Klak, C., G. Reeves, and T. Hedderson. 2004. Unmatched tempo of evolution in Southern African semi-desert ice plants. Nature 427:63–65.

Kluge, A. G. 1989. A concern for evidence and a phylogenetic hypothesis for relationships among *Epicrates* (Boidae, Serpentes). Syst. Zool. 38: 7–25.

Lanfear, R., B. Calcott, S. Y. W. Ho, and S. Guindon. 2012. PartitionFinder: combined selection of partitioning schemes and substitution models for phylogenetic analyses. Mol. Biol. Evol. 29:1695–1701.

Lengyel, S., A. D. Grove, A. M. Latimer, J. D. Majer, and R. R. Dunn. 2009. Ants sow the seeds of global diversification in flowering plants. PLoS ONE 5:e5480. doi:10.1371/journal.pone.0005480

Lewis, P. O. 2001. A likelihood approach to estimating phylogeny from discrete morphological character data. Syst. Biol. 50:913–925.

Lüttge, U. 2004. Ecophysiology of crassulacean acid metabolism (CAM). Ann. Bot. 93:629–652.

———. 2007. Physiological ecology. Pp. 187–234 *in* U. Lüttge, ed. *Clusia*: a woody Neotropical genus with remarkable plasticity and diversity. Springer-Verlag, Berlin, Germany.

Maddison, W. P., and D. R. Maddison. 2011. Mesquite: a modular system for evolutionary analysis. Version 2.75. Available at http://mesquiteproject.org

Maddison, W. P., P. E. Midford, and S. P. Otto. 2007. Estimating a binary character's effect on speciation and extinction. Syst. Biol. 56:701–710.

Magallón, S., and A. Castillo. 2009. Angiosperm diversification through time. Am. J. Bot. 96:349–365.

McWilliams, E. L. 1970. Comparative rates of dark CO_2 uptake and acidification in the Bromeliaceae, Orchidaceae, and Euphorbiaceae. Bot. Gaz. (Lond.) 131:285–290.

Mooney, H. A., J. H. Troughton, and J. A. Berry. 1977. Carbon isotope ratio measurements of succulent plants in southern Africa. Oecologia 30: 295–305.

O'Leary, M. H. 1988. Carbon isotopes in photosynthesis. BioScience 38:328–336.

Osborne, C. P., and D. J. Beerling. 2006. Nature's green revolution: the remarkable evolutionary rise of C_4 plants. Proc. R. Soc. Lond. B 361:173–194.

Osborne, C. P., and L. Sack. 2012. Evolution of C_4 plants: a new hypothesis for an interaction of CO_2 and water relations mediated by plant hydraulics. Philos. Trans. R. Soc. Lond. B 367:583–600.

Pagani, M., J. C. Zachos, K. H. Freeman, B. Tipple, and S. Bohaty. 2005. Marked decline in atmospheric carbon dioxide concentrations during the Paleogene. Science 309:600–603.

Pagel, M. 1999. The maximum likelihood approach to reconstructing ancestral character states of discrete characters on phylogenies. Syst. Biol. 48:612–622.

Partridge, T. C. 1993. The evidence for Cainozoic aridification in southern Africa. Quatern. Int. 17:105–110.

Pau, S., E. J. Edwards, and C. J. Still. 2013. Improving our understanding of environmental controls on the distribution of C_3 and C_4 grasses. Glob. Change Biol. 19:184–196.

Pearcy, R. W., and J. Troughton. 1975. C_4 photosynthesis in tree form *Euphorbia* species from Hawaiian rainforest sites. Plant Physiol. 55:1054–1056.

Peirson, J. A., P. V. Bruyns, R. Riina, J. J. Morawetz, and P. E. Berry. 2013. A molecular phylogeny and classification of the largely succulent and mainly African *Euphorbia* subg. *Athymalus* (Euphorbiaceae). Taxon 62: 1179–1200.

Pierce, S., K. Winter, and H. Griffiths. 2002. Carbon isotope ratio and the extent of daily CAM use by Bromeliaceae. New Phytol. 156:75–83.

Pittermann, J., S. A. Stuart, T. E. Dawson, and A. Moreau. 2012. Cenozoic climate change shaped the evolutionary ecophysiology of the Cupressaceae conifers. Proc. Natl. Acad. Sci. USA 109:9647–9652.

Pound, M. J., A. M. Haywood, U. Salzmann, and J. B. Riding. 2012. Global vegetation dynamics and latitudinal temperature gradients during the Mid to Late Miocene (15.97–5.33 Ma). Earth Sci. Rev. 112:1–22.

Prenner, G., and P. J. Rudall. 2007. Comparative ontogeny of the cyathium in *Euphorbia* (Euphorbiaceae) and its allies: exploring the organ-flower-inflorescence boundary. Am. J. Bot. 94:1612–1629.

Rabosky, D. L. 2010. Extinction rates should not be estimated from molecular phylogenies. Evolution 64:1816–1824.

Rabosky, D. L., and A. R. McCune. 2010. Reinventing species selection with molecular phylogenies. Trends Ecol. Evol. 25:68–74.

Rabosky, D. L., S. C. Donnellan, A. L. Talaba, and I. J. Lovette. 2007. Exceptional among lineage variation in diversification rates during the radiation of Australia's most diverse vertebrate clade. Proc. R. Soc. Lond. B 274:2915–2923.

Rambaut, A., and M. Charleston. 2002. TreeEdit. Phylogenetic tree editor, ver. 1.0 alpha 10. Available at http://tree.bio.ed.ac.uk/software/treeedit/

Rambaut, A., and A. J. Drummond 2007. Tracer, version 1.5. Univ. of Oxford, Oxford, U.K. Available at http://tree.bio.ed.ac.uk/software/tracer/

Riina, R., and P. E. Berry (coordinators). 2013. *Euphorbia* Planetary Biodiversity Inventory Project. Available at www.euphorbiaceae.org

Riina, R., J. A. Peirson, D. V. Geltman, J. Molero, B. Frajman, A. Pahlevani, L. Barres, J. J. Morawetz, Y. Salmaki, S. Zarre, et al. 2013. A worldwide molecular phylogeny and classification of the leafy spurges, *Euphorbia* subgenus *Esula* (Euphorbiaceae). Taxon 62:316–342.

Ruddiman, W. F., and J. E. Kutzbach. 1989. Forcing of late Cenozoic northern hemisphere climate by plateau uplift in southern Asia and the American west. J. Geophys. Res. Atmos. 94:18409–18427.

Sage, R. F. 2002. Are crassulacean acid metabolism and C_4 photosynthesis incompatible? Funct. Plant Biol. 29:775–785.

———. 2004. The evolution of C_4 photosynthesis. New Phytol. 161:341–370.

Sage, R. F., P.-A. Christin, and E. J. Edwards. 2011a. The C_4 plant lineages of planet Earth. J. Exp. Bot. 62:3155–3169.

Sage, T. L., R. F. Sage, P. J. Vogan, B. Rahman, D. C. Johnson, J. C. Oakley, and M. A. Heckel. 2011b. The occurrence of C_2 photosynthesis in *Euphorbia* subgenus *Chamaesyce* (Euphorbiaceae). J. Exp. Bot. 62:3183–3195.

Sanderson, M. J. 1997. A non-parametric approach to estimating divergence times in the absence of rate constancy. Mol. Biol. Evol. 14:1218–1231.

Santini, F., L. J. Harmon, G. Carnevale, and M. E. Alfaro. 2009. Did genome duplication drive the origin of teleosts? A comparative study of diversification in ray-finned fishes. BMC Evol. Biol. 9:194. doi:10.1186/1471-2148-9-194

Schluter, D., T. Price, A. O. Mooers, and D. Ludwig. 1997. Likelihood of ancestor states in adaptive radiation. Evolution 51:1699–1711.

Schwarz, G. 1978. Estimating the dimension of a model. Ann. Stat. 6:461–464.

Sepulchre, P., G. Ramstein, F. Fluteau, M. Schuster, J.-J. Tiercelin, and M. Brunet. 2006. Tectonic uplift and eastern Africa aridification. Science 313:1419–1423.

Shaw, A. J., N. Devos, C. J. Cox, S. B. Boles, B. Shaw, A. M. Buchanan, L. Cave, and R. Seppelt. 2010. Peatmoss (*Sphagnum*) diversification associated with Miocene Northern Hemisphere climatic cooling? Mol. Phylogenet. Evol. 55:1139–1145.

Silvera, K., L. S. Santiago, and K. Winter. 2005. Distribution of crassulacean acid metabolism in orchids of Panama: evidence of selection for weak and strong modes. Funct. Plant Biol. 32:397–407.

Silvera, K., K. M. Neubig, M. W. Whitten, N. H. Williams, K. Winter, and J. C. Cushman. 2010. Evolution along the crassulacean acid metabolism continuum. Funct. Plant Biol. 37:995–1010.

Silvestro, D., G. Zizka, and K. Schulte. 2014. Disentangling the effects of key innovations on the diversification of Bromelioideae (Bromeliaceae). Evolution 68:163–175.

Simpson, G. G. 1953. The major features of evolution. Columbia Univ. Press, New York, NY.

Slater, G. J., S. A. Price, F. Santini, and M. E. Alfaro. 2010. Diversity versus disparity and the radiation of modern cetaceans. Proc. R. Soc. Lond. B 277: 3097–3104.

Smith, J. A. C., and K. Winter. 1996. Taxonomic distribution of crassulacean acid metabolism. Pp. 427–436 *in* K. Winter and J. A. C. Smith, eds. Crassulacean acid metabolism: biochemistry, ecophysiology and evolution. Springer, New York, NY.

Smith, S. A., J. M. Beaulieu, A. Stamatakis, and M. J. Donoghue. 2011. Understanding angiosperm diversification using small and large phylogenetic trees. Am. J. Bot. 98:404–414.

Spriggs, E. L., P. -A. Christin, and E. J. Edwards. 2014. C_4 photosynthesis promoted species diversification during the Miocene grassland expansion. PLoS ONE 9:e97722. doi:10.1371/journal.pone.0097722

Stadler, T. 2009. On incomplete sampling under birth-death models and connections to the sampling-based coalescent. J. Theor. Biol. 261:58–66.

Steinmann, V. W., and J. M. Porter. 2002. Phylogenetic relationships in Euphorbieae (Euphorbiaceae) based on ITS and *ndhF* sequence data. Ann. Mo. Bot. Gard. 89:453–490.

Suc, J.-P. 1984. Origin and evolution of the Mediterranean vegetation and climate in Europe. Nature 307:429–432.

Suzuki, N., and S. Teranishi. 2005. Phenology and life cycle of the annual *Chamaesyce maculata* (L.) Small (Euphorbiaceae), with multiple overlapping generations in Japan. Ecol. Res. 20:425–432.

Tripati, A. K., C. D. Roberts, and R. A. Eagle. 2009. Coupling of CO_2 and ice sheet stability over major climate transitions of the last 20 million years. Science 326:1394–1397.

Valente, L. M., A. W. Britton, M. P. Powell, A. S. T. Papadopulos, P. M. Burgoyne, and V. Savolainen. 2014. Correlates of hyperdiversity in southern African ice plants (Aizoaceae). Bot. J. Linn. Soc. 174:110–129.

Vamosi, J. C., and S. M. Vamosi. 2011. Factors influencing diversification in angiosperms: at the crossroads of intrinsic and extrinsic traits. Am. J. Bot. 98:460–471.

van Ee, B. W., P. E. Berry, R. Riina, and J. E. G. Amaro. 2008. Molecular phylogenetics and biogeography of the Caribbean-centered *Croton* subgenus *Moacroton* (Euphorbiaceae s.s.). Bot. Rev. 74:132–165.

Verboom, A., J. K. Archibald, F. T. Bakker, D. U. Bellstedt, F. Conrad, L. L. Dreyer, F. Forest, C. Galley, P. Goldblatt, J. F. Henning, et al. 2009. Origin and diversification of the Greater Cape flora: ancient species repository, hot-bed of recent radiation, or both? Mol. Phylogenet. Evol. 51:44–53.

Vrba, E. S. 1984. What is species selection? Syst. Zool. 33:318–328.

Webster, G. L. 1967. The genera of Euphorbiaceae in the southeastern United States. J. Arnold Arb. 48:303–361, 363–430.

Webster, G. L., W. V. Brown, and B. N. Smith. 1975. Systematics of photosynthetic carbon fixation pathways in *Euphorbia*. Taxon 24:27–33.

Wells, N. A. 2003. Some hypotheses on the Mesozoic and Cenozoic paleoenvironmental history of Madagascar. Pp. 16–34 *in* S. M. Goodman and J. P. Benstead, eds. The natural history of Madagascar. Univ. of Chicago Press, Chicago, IL.

West-Eberhard, M. J. 2003. Developmental plasticity and evolution. Oxford Univ. Press, New York, NY.

Winter, K. 1979. $\delta^{13}C$ values of some succulent plants from Madagascar. Oecologia 40:103–112.

Winter, K., and J. A. M. Holtum. 2002. How closely do the $\delta^{13}C$ values of CAM plants reflect the proportion of CO_2 fixed during day and night? Plant Physiol. 129:1843–1851.

———. 2011. Induction and reversal of crassulacean acid metabolism in *Calandrinia polyandra*: effects of soil moisture and nutrients. Funct. Plant Biol. 38: 576–582.

Winter, K., J. Aranda, and J. A. M. Holtum. 2005. Carbon isotope composition and water-use efficiency in plants with crassulacean acid metabolism. Funct. Plant Biol. 32:381–388.

Winter, K., M. Garcia, and J. A. M Holtum. 2008. On the nature of facultative and constitutive CAM: environmental and developmental control of

CAM expression during early growth of *Clusia*, *Kalanchoë*, and *Opuntia*. J. Exp. Bot. 59:1829–1840.

Xi, Z., B. R. Rhufel, H. Schaefer, A. M. Amorim, M. Sugumaran, K. J. Wurdack, P. K. Endress, M. L. Mathews, P. F. Stevens, S. Mathews, et al. 2012. Phylogenomics and *a posteriori* data partitioning resolve the Cretaceous angiosperm radiation Malpighiales. Proc. Natl. Acad. Sci. USA 109:17519–17524.

Yang, Y., and P. E. Berry. 2011. Phylogenetics of the Chamaesyce clade (*Euphorbia*, Euphorbiaceae): reticulate evolution and long-distance dispersal in a prominent C_4 lineage. Am. J. Bot. 98:1486–1503.

Yang, Y., R. Riina, J. J. Morawetz, T. Haevermans, X. Aubriot, and P. E. Berry. 2012. Molecular phylogenetics and classification of *Euphorbia* subgenus *Chamaesyce* (Euphorbiaceae). Taxon 61:764–789.

Yoder, J. B., E. Clancey, S. Des Roches, J. M. Eastman, L. Gentry, W. Godsoe, T. J. Hagey, D. Jochimsen, B. P. Oswald, J. Robertson, et al. 2010. Ecological opportunity and the origin of adaptive radiations. J. Evol. Biol. 23:1581–1596.

Zachos, J., M. Pagani, L. Sloan, E. Thomas, and K. Billups. 2001. Trends, rhythms, and aberrations in global climate 65 Ma to present. Science 292:686–693.

Zimmermann, N. F. A., C. M. Ritz, and F. H. Hellwig. 2010. Further support for the phylogenetic relationships within *Euphorbia* L. (Euphorbiaceae) from nrITS and *trnL–trnF* IGS sequence data. Plant Syst. Evol. 286:39–58.

Zwickl, D. J. 2006. Genetic algorithm approaches for the phylogenetic analysis of large biological sequence datasets under the maximum likelihood criterion. Ph.D. dissertation, University of Texas at Austin, Austin, TX. Available at https://www.nescent.org/wg_garli/Main_Page

Associate Editor: V. Savolainen

Supporting Information

Additional Supporting Information may be found in the online version of this article at the publisher's website:

Supplemental Methods

Figure S1. Ninety-five percent majority-rule consensus tree of pool of all post burn-in trees from Bayesian MCMC analysis using MrBayes version 3.2.1 with the 197-tip dataset (15-partiton scheme; see Table S2); posterior probability values (PP) ≥ 0.95 are indicated above branches.

Figure S2. Chronogram (maximum clade credibility tree) inferred from the BEAST analysis of the 197-tip dataset of *Euphorbia* and outgroups (15-partition scheme; see Table S2).

Figure S3. Histogram plot of $\delta^{13}C$ values for *Euphorbia* and outgroups.

Figure S4. Ancestral state reconstructions of photosynthetic pathway type (C_3-like, with atmospheric CO_2 predominantly fixed by RuBisCO, or CCM with CO2 principally fixed by PEPCase).

Figure S5. Ancestral state reconstructions of photosynthetic pathway type (C_3-like, with atmospheric CO_2 predominantly fixed by RuBisCO, or CCM with CO2 principally fixed by PEPCase).

Figure S6. Density plot of the number of piecewise models fit to the 1000, 104-tip diversity trees in the MEDUSA analysis of *Euphorbia* and outgroups.

Figure S7. Posterior probability distributions of the net diversification rate of speciation rate (λ), extinction rate (μ), and character state transition rate (q) for *Euphorbia* and outgroups estimated from a Bayesian MCMC analysis the confidence set of BiSSE submodels.

Table S1. GenBank accession numbers for DNA sequences of the 23 *Euphorbia* species added to the matrix of Horn et al. (2012).

Table S2. Best-fit, 15-partition scheme and corresponding models of evolution for the 10-marker, 197-tip dataset of *Euphorbia* and outgroups selected using BIC from analysis with the "greedy" heuristic search algorithm in PartitionFinder version 1.0.1.

Table S3. Values of $\delta^{13}C$ and associated voucher information for taxa of *Euphorbia* and outgroups included in the 197-tip dataset.

Table S4. Clade tip diversity estimates used in the 104-tip MEDUSA and BiSSE analyses, and character state codings used in BiSSE analyses.

Table S5. Clades in which a significant shift in the net diversification rate (r) was modeled in 10–50% of the 1000 diversity trees using the MEDUSA method.